Published for SISSA by Springer

Received: *April 12, 2026*
Accepted: *June 18, 2026*
Published: *August 12, 2026*

A search for microscopic black holes, string balls, and sphalerons in proton-proton collisions at $\sqrt{s} = 13$ TeV



The CMS collaboration

Full author list at the end of the paper

E-mail: cms-publication-committee-chair@cern.ch

Abstract: A search for microscopic black holes, string balls, and electroweak sphalerons using proton-proton collisions at $\sqrt{s} = 13$ TeV recorded with the CMS detector at the CERN LHC during the 2016–2018 data taking, and corresponding to an integrated luminosity of 138 fb^{-1}, is presented. Two search strategies based on control samples in data are used. Model-independent limits on the cross section of physics phenomena with multiple energetic jets, leptons, and photons are set using a method that relies on the shape invariance of the scalar sum of the transverse momenta of all objects in the event. Model-dependent limits on black hole and sphaleron production are set using a newly introduced method that has been developed for the identification of collider events with distinct kinematic features by separating them into classes based on phase space proximity. In the context of models with large extra dimensions, semiclassical black holes and string balls with masses below 8.4–11.4 TeV and 9.0–10.7 TeV, respectively, are excluded at 95% confidence level, significantly extending the reach beyond previous searches. Results of a dedicated search for electroweak sphalerons are used to derive an upper limit of 0.0034 at 95% confidence level on the fraction of quark-quark interactions, with a center-of-mass energy above the nominal sphaleron transition energy threshold of 9 TeV, that result in a sphaleron transition.

Keywords: Beyond Standard Model, Hadron-Hadron Scattering

ArXiv ePrint: 2604.10732

Open Access, © The Authors.
Article funded by SCOAP^3.

https://doi.org/10.1007/JHEP08(2026)098

JHEP08(2026)098

Contents

1 Introduction **1**

2 The CMS detector **3**

3 Data and simulated samples **3**

4 Event reconstruction **5**

5 Observables **7**

5.1 Scalar sum of transverse momenta 7

5.2 Sphericity 7

5.3 Phase space distance 8

6 Event selection **9**

7 Background prediction methods **11**

7.1 Shape invariance method 11

7.2 Phase space distance method 12

8 Systematic uncertainties **14**

9 Results **15**

9.1 Model-independent results 15

9.2 Model-dependent results 17

10 Summary **19**

The CMS collaboration **28**

JHEP08(2026)098

1 Introduction

This paper describes a search for three theoretical objects predicted to exist at the TeV scale: microscopic black holes (BHs), string balls (SBs), and sphalerons. Microscopic BHs are the manifestation of certain theoretical scenarios beyond the standard model (BSM) that could address open questions of the standard model (SM), such as the hierarchy problem. The Arkani-Hamed–Dimopoulos–Dvali (ADD) [1–3] and Randall–Sundrum (RS) [4, 5] models address the hierarchy problem by means of extra dimensions with properties that can explain gravity's apparent weakness in the standard 3+1 dimensions of space-time. In this paper, we present the results of a search for manifestations of the ADD model. In this framework, the strength of gravity is greatly increased when its extra dimensional components are taken into account. This shifts the fundamental Planck scale (M_{D}) downward to a level near the electroweak (EW) scale. As a result, microscopic BH formation becomes possible for BHs with mass $M_{\mathrm{BH}} \geq M_{\mathrm{D}}$ [6–8]. In the semiclassical case where M_{BH} is well above M_{D}, the microscopic BHs quickly evaporate via Hawking radiation [9] to a large number of energetic particles, such as gluons, quarks, leptons, and photons. If M_{BH} is close to M_{D}, quantum effects become significant, altering the decays. For example, quantum BHs decay before they thermalize and produce low-multiplicity final states [10–12].

Another model based on string theory predicts that in the region between M_{D} and the threshold for BH formation, highly excited long, jagged SB states [13] can be produced with masses of order $M_{\mathrm{S}}/g_{\mathrm{S}}$, where M_{S} is the string scale and g_{S} is the string coupling. The transition from SBs to semiclassical BHs occurs for masses above $M_{\mathrm{S}}/g_{\mathrm{S}}^2$. Similar to semiclassical BHs, SB evaporation yields a large number of SM particles.

Sphalerons are unstable solutions of the electroweak field equations corresponding to saddle-point configurations of the electroweak potential [14, 15] that allow baryon and lepton number violation, an essential requirement for the matter-antimatter asymmetry in the universe. In the SM, there are twelve globally conserved currents $J^{\mu} = \overline{\psi}_{\mathrm{L}}\gamma^{\mu}\psi_{\mathrm{L}}$, each corresponding to the flavor conservation of one of the 12 fundamental fermions. When the conservation is broken by the electroweak chiral anomaly, the integral of the divergence of these currents over space-time produces what is known as the Chern–Simons number [15], N_{CS}, which characterizes the topological structure of the EW vacuum. Each sphaleron-induced transition is associated with an N_{CS}, resulting in a violation of baryon (B) and lepton (L) numbers by $\Delta B = \Delta L = 3N_{\mathrm{CS}}$, such that $\Delta(B+L) = 6N_{\mathrm{CS}}$ and $\Delta(B-L) = 0$. The sphaleron potential is a periodic potential with minima (the vacua) characterized by the integer values of N_{CS}. The energy required to overcome the potential barriers between minima, known as the sphaleron transition energy (E_{sph}), is estimated to be around 9 TeV [16]. An anomaly only occurs when there is sufficient energy to overcome the potential barrier. The minimal final state from a sphaleron transition, corresponding to $N_{\mathrm{CS}} = \pm 1$, consists of 12 fermions: three charged leptons, three neutrinos, and six quarks (one from each generation and color). Additional quark-antiquark pairs and gauge bosons may also be produced in the process, leading to high-multiplicity final states, potentially observable at the CERN LHC [16–18].

At the LHC, three types of objects discussed above could produce very similar event signatures involving multiple leptons, photons, and jets that are distinct from SM backgrounds.

The ATLAS Collaboration published a search for BHs [19] using 3.6 fb^{-1} of data collected at $\sqrt{s} = 13$ TeV that was recast by Ellis and Sakurai as a search for sphalerons [17]. The ATLAS Collaboration also searched for quantum BHs in lepton+jet final states using a $\sqrt{s} = 13$ TeV data set corresponding to an integrated luminosity of 140 fb^{-1} [20]. An analysis by CMS at the same center-of-mass energy, based on 2016 data, corresponding to an integrated luminosity of 35.9 fb^{-1}, was reported in ref. [21]. The search reported here is an update to the previous CMS analysis. In addition to using a larger data set, we use a novel phase space metric to set model-dependent limits, while also applying the shape invariance approach used in previous CMS publications [21–25], to set model-independent limits.

The paper is organized as follows. The CMS detector and event reconstruction are presented in section 2. Section 3 describes the signal models considered and the associated simulated data samples. Section 4 discusses the event reconstruction, while section 5 introduces the variables used in this search. The event selection is detailed in section 6, followed in section 7 by descriptions of the two background estimation methods we employ. Section 8 presents the systematic uncertainties associated with the signal simulation, and the results are shown in section 9. The paper is summarized in section 10.

Tabulated results are provided in the HEPData record for this analysis [26].

JHEP08(2026)098

2 The CMS detector

The central feature of the CMS apparatus is a superconducting solenoid of 6 m internal diameter, providing a magnetic field of 3.8 T. Within the solenoid volume are a silicon pixel and silicon strip tracker, a lead tungstate crystal electromagnetic calorimeter (ECAL), and a brass and scintillator hadron calorimeter (HCAL), each composed of a barrel and two endcap sections. Forward calorimeters extend the pseudorapidity (η) coverage provided by the barrel and endcap detectors. Muons are measured in gas-ionization detectors embedded in the steel flux-return yoke outside the solenoid. A more detailed description of the CMS detector, together with a definition of the coordinate system used and the relevant kinematic variables, can be found in refs. [27, 28].

The silicon tracker used in 2016 measured charged particles within the range $|\eta| < 2.5$. For nonisolated particles of transverse momenta (p_{T}) between 1 and 10 GeV, and $|\eta| < 1.4$, the track resolutions were typically 1.5% in p_{T} and 25–90 (45–150) μm in the transverse (longitudinal) impact parameter [29]. At the start of 2017, a new pixel detector was installed [30]; the upgraded tracker measured particles up to $|\eta| = 3.0$ with typical resolutions of 1.5% in p_{T} and 20–75 μm in the transverse impact parameter [31] for nonisolated particles of $1 < p_{\mathrm{T}} < 10$ GeV. According to simulation studies [32], similar improvements are expected in the longitudinal direction.

Events of interest are selected by a two-level trigger system. The first level, composed of custom hardware processors, uses information from the calorimeters and muon detectors to select events at a rate of approximately 100 kHz within a fixed latency of approximately 4 μs [33]. The second level, known as the high-level trigger (HLT), consists of a farm of processors running a version of the full event reconstruction software optimized for fast processing. It reduces the event rate to a few kHz before data storage [34, 35].

3 Data and simulated samples

The analysis is based on a data sample collected with the CMS detector from 2016 to 2018 in proton-proton (pp) collisions at a center-of-mass energy of 13 TeV, corresponding to an integrated luminosity of 138 fb^{-1}.

The BH signal samples were produced at leading order using Monte Carlo (MC) simulation with the BlackMax v2.02.0 [36] and Charybdis2 v1.003 [37, 38] generators at $\sqrt{s} = 13$ TeV. The Charybdis2 generator models BH decay primarily through semiclassical Hawking radiation with graybody factors, while BlackMax offers more flexible parameterizations for the decay spectra and different treatments of mass and angular momentum loss during evaporation. The SB samples were generated using Charybdis2. The sphaleron samples used the BaryoGEN v1.0 [39] generator. Simulations for quantum chromodynamics (QCD) multijet production with MadGraph5_aMC@NLO v2.2.2 [40] at leading order using the MLM matching scheme [41] have been employed to guide the selection criteria and train machine-learning models, as detailed in section 6.

JHEP08(2026)098

The BH samples were produced under different assumptions regarding the angular momentum, energy loss, and decay mechanisms. Samples labeled with "B" were produced using the BlackMax generator:

- B1: nonrotating;
- B2: rotating with no graviton emission included;
- B3: rotating with energy and angular momentum loss (graviton emission included);

while those labeled with "C" were produced using the Charybdis2 generator:

- C1: rotating;
- C2: nonrotating;
- C3: rotating with the evaporation model in refs. [42, 43];
- C4: rotating with the Yoshino–Rychkov (YR) loss model [44], which is a conservative bound that includes impact parameter considerations;
- C5: rotating, stable-remnant model [45–47], where the stable remnant must be a colorless object essentially equivalent to a quark-antiquark bound state;
- C6: rotating, boiling remnant model [13, 48], where the remnant continues to evaporate until a maximum Hawking temperature equal to M_{D} is reached.

Furthermore, the samples were simulated with various combinations of model parameters. For each model, the fundamental Planck scale M_{D} is varied between 2 and 9 TeV in 1 TeV steps and for every mass value, n = 2, 4, and 6 extra dimensions are used. The number of extra dimensions corresponds to representative benchmarks commonly used in previous searches and spans a broad range of phenomenologically relevant models. The parameter grids are chosen to provide adequate coverage of the accessible phase space while maintaining a manageable number of simulated samples. The signal model varies smoothly between neighboring simulated mass points, making interpolation between them appropriate. This procedure was validated by comparing limits obtained from interpolated signal templates at intermediate mass points with those obtained by interpolating between limits at neighboring simulated mass points, yielding very similar results. As BH production is a threshold phenomenon, we search for BHs above a certain minimum mass $M_{\mathrm{BH}}^{\mathrm{min}}$. We vary $M_{\mathrm{BH}}^{\mathrm{min}}$ in simulation from $(M_{\mathrm{D}} + 1)$ TeV to 12 TeV in 1 TeV steps.

The production of SBs depends on two parameters, the string scale M_{S} and the string coupling g_{S}. For all SB samples, $n = 6$ is used. In weakly-coupled string scenarios compactified to $4 + n$ dimensions, M_{D} and the string parameters are related by [48],

$$M_{\mathrm{D}} = g_{\mathrm{S}}^{-\left(\frac{2}{n-2}\right)} M_{\mathrm{S}}. \tag{3.1}$$

In simulation, the string scale M_{S} is varied from 1 to 4 TeV in 0.5 TeV steps. For each mass value, g_{S} values of 0.2, 0.3, and 0.4 are used, while the minimum mass of SBs ranges from

JHEP08(2026)098

7 to 12 TeV in steps of 1 TeV. These parameter ranges cover both the formation of SBs and their transition to semiclassical BHs.

Sphaleron production depends on two parameters, E_{sph} and N_{CS}. The parameter E_{sph} is scanned in a range from 8.5 to 9.5 TeV in steps of 0.25 TeV. Since the sphaleron transition is exponentially suppressed by $|N_{\text{CS}}|$, only $N_{\text{CS}} = \pm 1$ are simulated. The probability of $N_{\text{CS}} = +1$ is denoted as $p(N_{\text{CS}})$. The $p(N_{\text{CS}})$ values of 0%, 50%, and 100% were used, where, for example, $p(N_{\text{CS}}) = 50\%$ means half of the events have $N_{\text{CS}} = +1$ and half have $N_{\text{CS}} = -1$.

The theoretical cross section for sphaleron production is calculated in terms of the partonic cross section [18],

$$\hat{\sigma}\left(\sqrt{\hat{s}}\right) = \frac{p_{\text{sph}}}{m_{\text{W}}^2}\Theta\left(\sqrt{\hat{s}} - E_{\text{sph}}\right), \tag{3.2}$$

where m_{W} is the mass of the W boson, $\hat{s}$ is the square of the partonic center-of-mass energy, and Θ is the Heaviside step function. The partonic cross section is parameterized by the two parameters E_{sph} and p_{sph}, where the latter is a dimensionless phenomenological pre-exponential factor that scales the reference sphaleron production cross section above the threshold E_{sph}. The sphaleron samples were generated assuming $p_{\text{sph}} = 1$, which facilitates setting a limit on this factor.

In all MC samples, PYTHIA v8.205 was used for hadronization with tune CP5 [49]. The parton distribution function (PDF) set used in simulation is NNPDF3.1 at next-to-next-to-leading order in perturbative QCD [50]. Simulated minimum bias events are superimposed on the primary collision to mimic the impact of additional interactions that occur in the same or adjacent bunch crossings (pileup) [51].

4 Event reconstruction

For this analysis, which focuses on searching for signals at the TeV scale, events are selected using an HLT criterion based on the scalar sum of transverse momenta of the reconstructed jets (H_{T}) in the event. The lowest H_{T} threshold that ensures optimal performance and data coverage is chosen. For data taken in the year 2016 this threshold is 900 GeV, while for 2017–2018 it is 1050 GeV. The resulting trigger selection is fully efficient for events that subsequently satisfy the offline requirements used in the analysis. Beyond the HLT requirement, a preselection of $S_{\text{T}} > 2$ TeV is applied, where S_{T} is defined as the scalar sum of the transverse momenta of all reconstructed objects in the event. The subsequent requirements described in this section define the full event selection used in the analysis, for which particles are reconstructed using the particle-flow (PF) algorithm [52].

The PF algorithm aims to identify each individual particle in an event, with an optimized combination of information from the various elements of the CMS detector. The energy of photons is obtained from the ECAL measurement. The energy of electrons is determined from a combination of the electron momentum at the primary interaction vertex as determined by the tracker, the energy of the corresponding ECAL cluster, and the energy sum of all bremsstrahlung photons spatially compatible with emission from the electron along its curved track. The energy of muons is obtained from the curvature of the corresponding track. The energy of charged hadrons is determined from a combination of their momentum measured in

JHEP08(2026)098

the tracker and the matching ECAL and HCAL energy deposits, corrected for the response function of the calorimeters to hadronic showers. Finally, the energy of neutral hadrons is obtained from the corresponding corrected ECAL and HCAL energies.

The primary vertex is taken to be the vertex corresponding to the hardest scattering in the event, evaluated using tracking information alone, as described in section 9.4.1 of ref. [53]. Events are required to contain a primary vertex within 24 cm of the nominal collision point along the beam axis and within 2 cm in the transverse direction.

Jets are clustered from PF particles using the anti-k_{T} algorithm with a distance parameter $R = 0.4$. The jet momentum is determined as the vectorial sum of all particle momenta in the jet, and is found from simulation to be within 5 to 10% of the true momentum over the whole p_{T} spectrum and detector acceptance. Jet energy corrections are derived from simulation to bring the average measured jet energy into agreement with that of particle-level jets. In situ measurements of the momentum balance in dijet, γ+jets, and Z+jets events are used to determine any residual differences between the jet energy scale in data and in simulation, and appropriate corrections are applied [54]. Pileup interactions can contribute additional tracks and calorimetric energy depositions to the jet momentum. To mitigate this effect, charged particles matched to pileup vertices are removed and an offset correction is applied to correct for remaining neutral-particle contributions [55]. All jets are required to have $p_{\mathrm{T}} > 70\,\mathrm{GeV}$, and pseudorapidity $|\eta| < 2.5$. The threshold of 70 GeV is chosen consistently for all reconstructed objects to ensure sufficient signal acceptance while preserving sensitivity across a wide range of signal samples. Additional selection criteria [56] are applied to each jet to remove those originating from calorimetric noise. An event-level filter is applied such that the energy fraction carried by muon candidates in the leading p_{T} jet that fails the standard identification must be less than 80%. This requirement removes events in which a low-momentum muon is misreconstructed with very high momentum and misidentified as a high-energy jet.

Electrons are reconstructed as charged-particle tracks with additional energy depositions in the ECAL [57]. A requirement of pseudorapidity $|\eta| < 2.5$ is applied to all electrons. Identification criteria make use of a discriminant that combines information on the reconstructed electron and its isolation from other activity in the event. Additional constraints on the transverse and longitudinal impact parameters of electron tracks ensure consistency with the primary vertex. The chosen discriminant working point corresponds to a selection efficiency of approximately 80% [58].

Photon reconstruction is based on information from the electromagnetic calorimeter with the requirement of no matched charged-particle tracks. As for electrons, a requirement of pseudorapidity $|\eta| < 2.5$ is applied along with an identification discriminant working point that achieves approximately 80% efficiency [58].

Muon candidates are reconstructed using the PF algorithm and are categorized as global muons [59], by the combined fit of tracks in the silicon tracker and the muon system. Tight selection criteria are then applied to remove misidentified muons from hadronic decays or hadron shower remnants [60]. An isolation requirement is applied to reduce contamination from nonprompt muons originating from decays of hadrons within jets. Muon candidates are required to have pseudorapidity $|\eta| < 2.4$.

JHEP08(2026)098

An object arbitration procedure is used to disambiguate objects in the event. It is applied to photons and jets using a cone centered on their reconstructed approximate trajectories, of size $\Delta R = \sqrt{(\Delta\eta)^2 + (\Delta\phi)^2} = 0.4$. The arbitration proceeds in a specific hierarchical order as follows. First, all leptons are retained. Next, photons are selected only if there is no lepton in the cone. Finally, jets are selected from the remaining objects, provided that there is no lepton or photon in the cone.

The missing transverse momentum vector $\vec{p}_{\mathrm{T}}^{\,\mathrm{miss}}$ is defined as the projection onto the plane perpendicular to the beam axis of the negative vector sum of the momenta of all reconstructed PF objects in an event [61]. Its magnitude is referred to as $p_{\mathrm{T}}^{\mathrm{miss}}$. The jet energy corrections are propagated into the $p_{\mathrm{T}}^{\mathrm{miss}}$ reconstruction.

5 Observables

The key observables used in this analysis to discriminate between signal and background include the scalar sum of transverse momenta of all objects in the event (S_{T}), sphericity (S) [62–64], and in the case of the model-dependent search, a novel phase space distance metric is also employed. The objects in an event are jets, electrons, photons, muons, and missing transverse momentum ($p_{\mathrm{T}}^{\mathrm{miss}}$).

5.1 Scalar sum of transverse momenta

The S_{T} variable is defined as the scalar sum of the p_{T} of all objects in the event,

$$S_{\mathrm{T}} = \left(\sum_{i=1}^{N} p_{\mathrm{T}i}\right) + p_{\mathrm{T}}^{\mathrm{miss}}. \tag{5.1}$$

The S_{T} distributions for various signal models, together with that of the QCD multijet background, are shown in figure 1 (left). Among BH signals, we use the B1 model with $n = 2$ and $M_{\mathrm{D}} = 2\,\mathrm{TeV}$ as a representative case for the description of the analysis, including many figures and resulting exclusions. Where relevant, figures focus on the M_{BH} and M_{D} mass points near exclusion. Other models are treated similarly and the limits associated with them are included in the final exclusion plots in section 9. For the sphaleron signal, the nominal $E_{\mathrm{sph}} = 9\,\mathrm{TeV}$ with different $p(N_{\mathrm{CS}})$ assumptions is shown.

The shape of the S_{T} distribution for background processes, which is dominated by QCD multijet background, is assumed to be independent of the object multiplicity, N. This facilitates the modeling of the background from control regions (CRs) and the extension of its prediction to higher multiplicities where BSM physics signals may be present. This is discussed in more detail in section 7.1.

5.2 Sphericity

Sphericity is a measure of how isotropic an event is, and it is employed to improve signal sensitivity. In this paper, sphericity is defined as follows:

$$S = \frac{2\lambda_2}{\lambda_2 + \lambda_1}, \tag{5.2}$$

JHEP08(2026)098

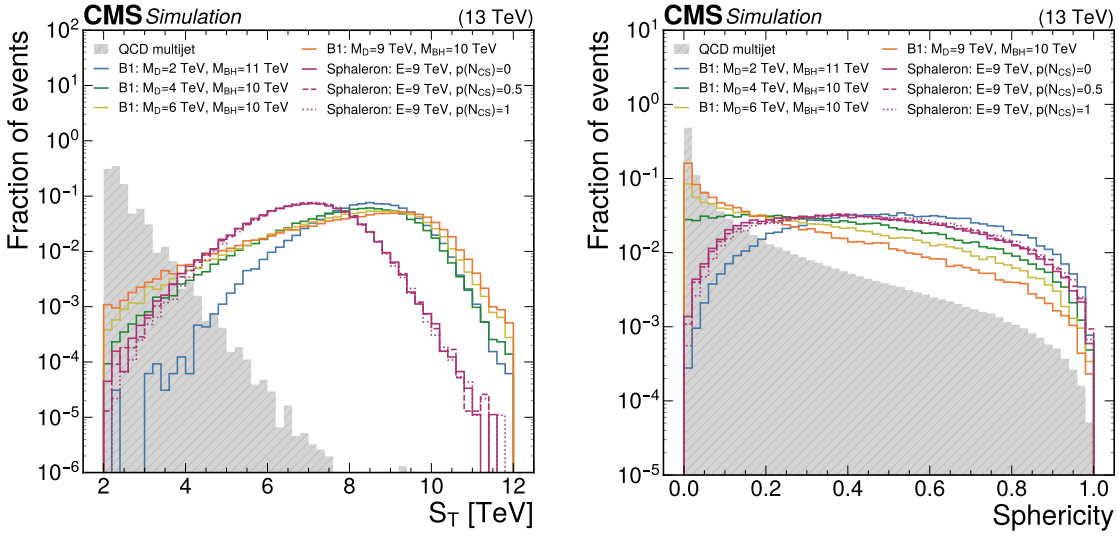


Figure 1. The S_{T} (left) and sphericity (right) distributions for various BH (with $n = 2$) and sphaleron signal models are plotted along with the corresponding distributions for simulated QCD multijet background events. The distributions are normalized to unit area.

where λ_1 and λ_2 are the eigenvalues of the transverse momentum tensor,

$$S_{xy}^{L} = \frac{1}{\sum_i p_{\mathrm{T}i}} \sum_i \frac{1}{p_{\mathrm{T}i}} \begin{bmatrix} p_{xi}^2 & p_{xi}p_{yi} \\ p_{xi}p_{yi} & p_{yi}^2 \end{bmatrix}, \tag{5.3}$$

where the index i extends over all objects passing our selection criteria. The definition of sphericity in this paper is restricted to the transverse plane and has been referred to as transverse sphericity [63, 64]. Signal events tend to be more spherical than background events due to the isotropic decays of BHs and sphalerons. Therefore, it is expected that the sphericity distribution for signal events will be shifted towards higher values compared to the QCD multijet background, as shown in figure 1 (right). As the mass of the BH increases, its temperature decreases, which results in a larger number of softer objects emitted in the process of evaporation. BH models with higher M_{BH} tend to have a more pronounced shift to higher sphericity values.

5.3 Phase space distance

Novel representations of collider data play an increasingly important role in modern machine learning methods. For example, optimal transport distances using energy flow distributions, have given rise to a new geometry of collider events [65–67] that has widespread applications in particle physics [68–72]. However, less attention has been given to the intrinsic geometry of the phase space manifold where scattering amplitudes are defined. A natural distance between collider events with N objects was proposed in ref. [73]. To this end, a covariant description of the massless N-body phase space manifold Π_N is presented and shown to be isomorphic to the product space of an $(N-1)$-simplex Δ_{N-1} and a $(2N-3)$-hypersphere S_{2N-3}: $\Pi_N \cong \Delta_{N-1} \otimes S_{2N-3}$. Explicit and global coordinates of the phase space, $\vec{\rho}$ for

JHEP08(2026)098

the simplex and $\vec{v}$ for the hypersphere, are obtained via transforms of the four-vectors of the N objects in the event.

A practical metric for collider events using global phase space coordinates was developed and tailored to the structure of events at hadron colliders in the center-of-mass frame [74]. After pre-processing the collider events and the manifold, the metric distance between two events, A and B, is defined by

$$d_{\Pi}(\vec{\rho}_{\mathrm{A}}, \vec{v}'_{\mathrm{A}}; \vec{\rho}_{\mathrm{B}}, \vec{v}'_{\mathrm{B}}) = \sqrt{\frac{1}{16\pi^2}\left(\frac{c}{4}\right)^{\frac{3-2N}{3N-4}} d^2_{\Delta}(\vec{\rho}_{\mathrm{A}}, \vec{\rho}_{\mathrm{B}}) + \frac{1}{4\pi^2}\left(\frac{c}{4}\right)^{\frac{N-1}{3N-4}} d^2_{\mathrm{S}}(\vec{v}'_{\mathrm{A}}, \vec{v}'_{\mathrm{B}})}, \tag{5.4}$$

where d_{Δ} is the distance on the simplex, d_{S} is the distance on the hypersphere, and c serves as a relative reweighting factor that gives rise to equally valid phase space distances. The relative reweighting factor is optimized to maximize the performance of the phase space distance in distinguishing signal from background events. In this analysis, we use the ratio sphere: simplex $= 4:1$, defined as the ratio of the coefficients that multiply the hypersphere term d^2_{S} and the simplex term d^2_{Δ} in eq. (5.4). For any object multiplicity N this ratio of coefficients reduces to c, so the choice $4:1$ corresponds to setting $c = 4$. The definitions of the coordinates and derivations of the distances can be found in ref. [74]. When combined with downstream machine-learning algorithms, the phase space distance achieves approximately 80% accuracy in distinguishing top quark pair production events from QCD dijet events in MC simulations.

Given that the dimension of the phase space manifold depends on the particle multiplicity N, a consistent means of defining the distance between events with different multiplicities is needed. In this work, we achieve this by fixing the number of objects per event to $N = 30$. This number covers the highest multiplicity seen in signal MC samples. When fewer than 30 objects are available in an event, the remaining entries are 'zero-padded', i.e., they are assigned a value of zero for subsequent calculations.

6 Event selection

A sphericity requirement of $S > 0.1$, is applied to reject background events, particularly at low S_{T}, where background contamination is highest. The sphericity requirement is determined from a scan of the sphericity threshold, evaluating the expected significance for all signal models considered. With the $S > 0.1$ selection, an average improvement in sensitivity of approximately 70% is observed across the signal models used in this search. While a small number of models show a mild reduction in significance, the majority of signal models have a substantial gain, with improvements up to ∼200%.

A preselection requirement of $N \geq 3$ objects is applied for the background fit in the model-independent search described in section 7.1, while $N \geq 4$ objects is required for the phase space distance method described in section 7.2.

Due to the high dimensionality of the phase space manifold, the phase space distance, defined in section 5, is not an optimal discriminator on its own and so it is combined with a machine-learning classifier to enhance the separation between signal and background. The support vector machine (SVM) [75] classifier is chosen for this purpose because of its efficacy in handling high-dimensional data and because of its intrinsic design that makes it a natural

JHEP08(2026)098

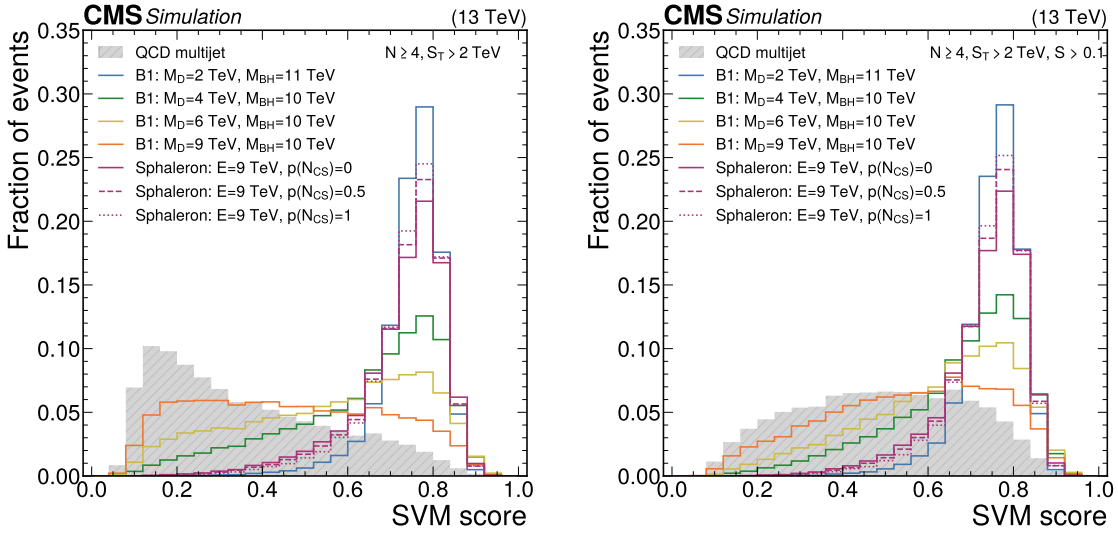


Figure 2. The SVM score distributions for simulated QCD multijets, and selected BH (with $n = 2$) and sphaleron models, before (left) and after (right) the sphericity requirement. The distributions are normalized to unit area.

choice for processing distance-based inputs. Using pairwise phase space distances as input, the SVM classifies events by constructing a maximum-margin hyperplane that maximizes the distance to the nearest data points from each class. This approach is more interpretable than a "black-box" neural network because the decision boundary (hyperplane) is constructed with physically motivated phase space distances. The radial basis function is used as the kernel to provide a non-linear generalization for the SVM classifier,

$$k(\vec{x}_{\mathrm{A}}; \vec{x}_{\mathrm{B}}) = \exp\left[-\gamma d(\vec{x}_{\mathrm{A}}; \vec{x}_{\mathrm{B}})^2\right], \tag{6.1}$$

where $d(\vec{x}_{\mathrm{A}}; \vec{x}_{\mathrm{B}}) = d_{\Pi}(\vec{\rho}_{\mathrm{A}}, \vec{v}'_{\mathrm{A}}; \vec{\rho}_{\mathrm{B}}, \vec{v}'_{\mathrm{B}})$ is the phase space distance between event A and event B, and γ is a hyperparameter that controls the width of the kernel, which is optimized during the validation step of the training. The SVM model provides a probability for how signal-like an event is, which is used as the SVM score in the subsequent analysis. To train the SVM, a simulated QCD multijet sample is used for background, and a mixture of mass points in the nonrotating B1 model with $n = 2$ extra dimensions is used as signal. This general model was evaluated on other signals, including sphalerons, and demonstrated good performance. This is likely because the B1 model with $n = 2$ is the most background-like, and so cases where the signal is further from the background in this metric are less challenging to distinguish.

Figure 2 shows the SVM score distributions normalized to equal area for simulated QCD multijet background and selected signal models, before (left) and after (right) the sphericity requirement.

The value of the SVM score used to define the final signal search region (SR) in data is optimized to maximize signal sensitivity as measured by the Punzi figure of merit [76] with $\sigma = 5$ and is found to be 0.63 for several signal models. To evaluate the stability of the results near this choice, the threshold was shifted to 0.5 or 0.7 resulting in a 4 to 25% variation in the yield of signal events, depending on the mass point.

JHEP08(2026)098

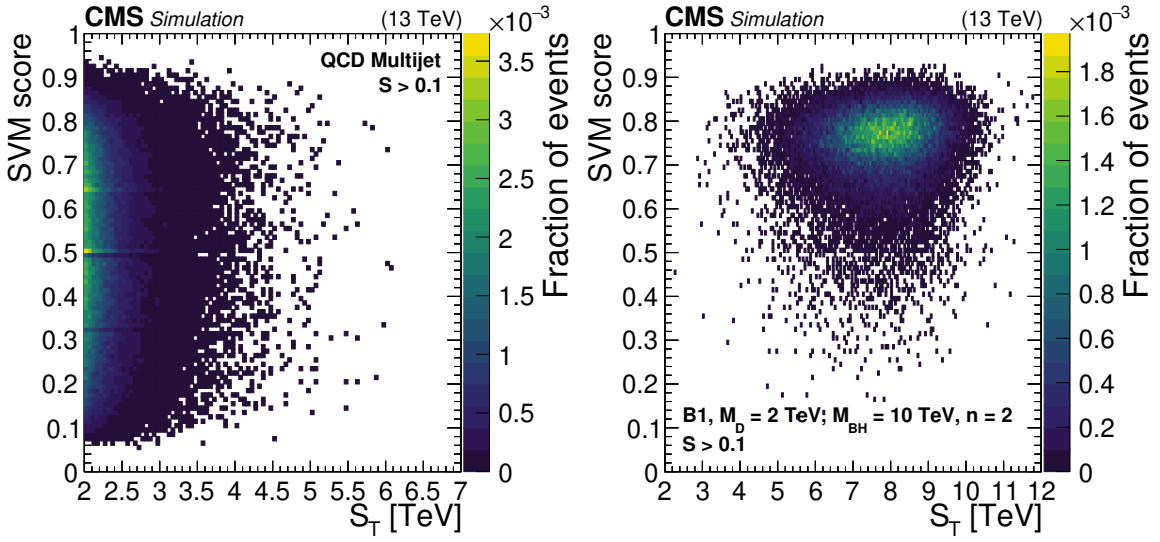


Figure 3. The SVM score vs. the S_{T} distributions for simulated QCD multijet background (left) and the BH signal model B1 with $M_{\mathrm{D}} = 2\,\mathrm{TeV}$, $M_{\mathrm{BH}} = 10\,\mathrm{TeV}$, and $n = 2$ (right), after the $S > 0.1$ selection.

Figure 3 shows distributions of SVM score versus S_{T} for simulated QCD multijet background events (left) and the BH signal model B1 with $M_{\mathrm{D}} = 2\,\mathrm{TeV}$, $M_{\mathrm{BH}} = 10\,\mathrm{TeV}$, and $n = 2$ (right). Clear separation between signal and background is observed.

7 Background prediction methods

The dominant background is expected to originate from QCD multijet events. The contribution from processes, like $\mathrm{t\bar{t}}$, W+jets or Z+jets, is found to be negligible. As noted above, the searches presented in this paper follow two different approaches. The two approaches also entail different background prediction methods.

7.1 Shape invariance method

The shape invariance (SI) approach, following previous CMS publications on this topic [21–25], assumes S_{T} invariance with respect to the multiplicity N, which allows for an estimate of the QCD background across samples selected with different minimum multiplicities. Simulation studies confirm that the shape of the S_{T} distribution remains consistent across multiplicities, allowing the use of low-multiplicity events to model the S_{T} distribution of high-multiplicity backgrounds. Deviations associated with initial-state radiation and the selection on sphericity are taken into account by additional systematic uncertainties, as described in section 8.

The method proceeds by first fitting 16 analytic functions to the S_{T} distribution from events with multiplicity $N = 3$ in a control region (SI-CR). These functional forms have been commonly used in previous searches to model the QCD S_{T} spectrum and are known to provide a good description of the data within the fit region. The SI-CR, which spans from $S_{\mathrm{T}} = 2.5\,\mathrm{TeV}$ to $S_{\mathrm{T}} = 5.2\,\mathrm{TeV}$, is optimized to ensure robust background estimation, while maintaining negligible signal contamination. To ensure a physically meaningful behavior of

JHEP08(2026)098

the background prediction, functions that do not exhibit a monotonically decreasing behavior over the relevant S_{T} range are excluded. All remaining candidate functions provide an acceptable description of the data in the SI-CR, as determined by goodness-of-fit tests. The choice of the nominal function is based on a comparison of the integrals of the candidate functions in the range $5 < S_T < 7\,\mathrm{TeV}$. The function whose integral is closest to the central value, defined as the average of the mean and median of the set of accepted functions, is selected as the nominal function. This function defines the nominal background shape prediction. The spread among the accepted functions is treated as a systematic uncertainty, as described in section 8. This function is then propagated to higher multiplicities of the final-state objects. The nominal function, chosen to be representative of the central behavior of the accepted function set, is given by

$$f(S_{\mathrm{T}}) = \frac{p_0\,(1-(S'_{\mathrm{T}})^{1/3})^{p_1}}{(S'_{\mathrm{T}})^{\,p_2+p_3\ln(S'_{\mathrm{T}})}}, \tag{7.1}$$

where $S'_{\mathrm{T}} = S_{\mathrm{T}}/\sqrt{s}$ and p_i $(i = 0, 1, 2, 3)$ are the fit parameters.

For each multiplicity threshold, the background estimate is normalized within a specific low-S_{T} window. The boundaries of this window are determined using simulated QCD multijet events. The window begins at the S_{T} value where the ratio relative to the exclusive $N = 3$ distribution reaches 99% of its plateau value. The exclusive $N = 3$ distribution refers to the fitted background function obtained from the 2.5–5.2 TeV range. The window then extends 400 GeV beyond this threshold, ensuring that there is a sufficient number of events in the normalization region. The regions of S_{T} between 2.5 and 5.2 TeV then serve as a validation region (SI-VR) to ensure that the background estimation works well in data. The S_{T} range directly above this region defines the signal region (SI-SR). Figure 4 shows that the prediction in SI-VR describes the data within the uncertainties for different multiplicity thresholds, including both low and high multiplicities.

7.2 Phase space distance method

The background prediction method for the phase space (PS) distance approach is the Alphabet method [77], which relies on control samples in data as described below.

First, the SVM score is used to define regions enriched in background and depleted of signal. The SR, referred to as the PASS region, contains events with SVM score greater than or equal to 0.63. The CR, also referred to as the FAIL region, is defined by the complementary set of events with a score smaller than 0.63. All events are required to satisfy $N \geq 4$ and $S > 0.1$ as discussed in the previous section.

Binned S_{T} distributions are then created for both PASS and FAIL regions. The background yields in the PASS region are estimated from the observed data distribution in the FAIL region, multiplied by a transfer function $R_{\mathrm{P/F}}(j)$,

$$N^{\mathrm{bkg}}_{\mathrm{PASS}}(j) = R_{\mathrm{P/F}}(j)\, N^{\mathrm{bkg}}_{\mathrm{FAIL}}(j), \tag{7.2}$$

where $N^{\mathrm{bkg}}_{\mathrm{PASS}}(j)$ is the estimated background yield in the j-th bin of the S_{T} distribution in the PASS region, $N^{\mathrm{bkg}}_{\mathrm{FAIL}}(j)$ is a floating parameter that determines the background yield

JHEP08(2026)098

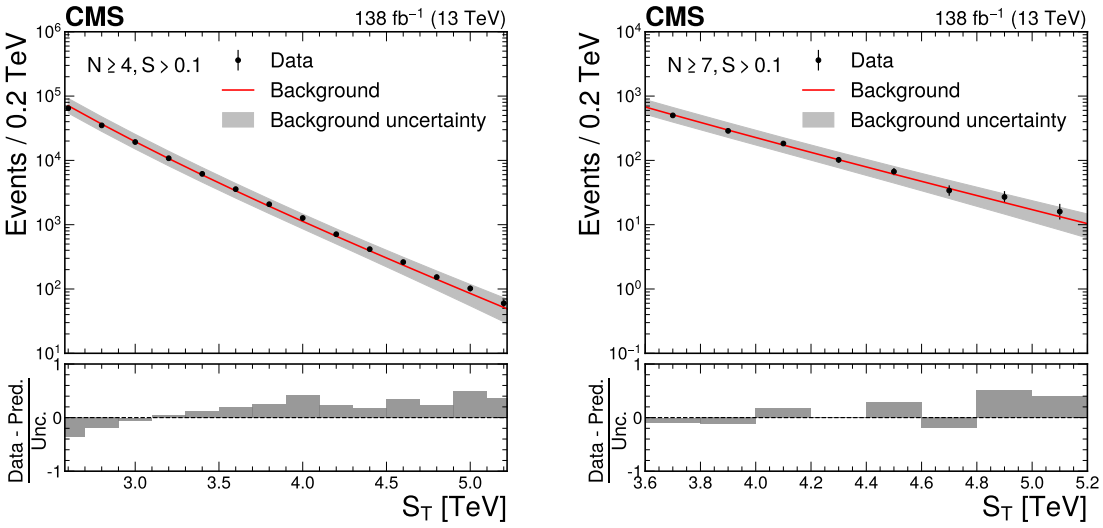


Figure 4. The S_T distribution in the $N \geq 4$ (left) and $N \geq 7$ (right) in the SI-VR in data is indicated by the black dots. The background prediction is represented by the red line, and the gray band corresponds to the background modeling uncertainty. The lower panels show the difference between observed data and the background prediction, normalized by the total uncertainty.

in the j-th bin of the S_T distribution in the FAIL region, which is constrained to values close to the observed data yield in the fit described below, and $R_{P/F}(j)$ is the value of the pass-to-fail ratio for bin j. The $R_{P/F}$ ratio is modeled by an exponential function to ensure a positive yield. Higher-order polynomials were found to have comparable performance when evaluated by the Fisher F-test [78, 79].

Finally, a binned maximum likelihood fit is performed simultaneously in the PASS and FAIL regions to extract both the background model, including the parameters of the $R_{P/F}(j)$ function and the binned background yield in the FAIL region, and the signal strength. All correlations between the parameters of the $R_{P/F}(j)$ function and the nuisance parameters are accounted for by construction.

The method performs well in tests with MC simulations. To test the method with data, a validation region (VR), defined by inverting the sphericity requirement to $S < 0.1$ is used. The VR-FAIL and VR-PASS regions are once again separated by the SVM score of 0.63. The post-fit distributions of the S_T variable in the VR-FAIL and VR-PASS regions are shown in the left and right plots of figure 5, respectively. The signal mass point B1, $M_D = 2\,\text{TeV}$, $M_{BH} = 10\,\text{TeV}$, and $n = 2$ is also shown in the plots and indicates that there is negligible signal contamination. The pull distributions in the PASS region, namely the distributions of the ratios plotted in the lower panels, are found to be approximately symmetrical, with standard deviations consistent with unity and centered near zero. The observed saturated log-likelihood p-value in the VR-PASS region is higher than 0.05, indicating good agreement between the background prediction and the data. The higher level of agreement between the model and the data in the VR-FAIL region arises because this region is used to constrain the background estimate.

JHEP08(2026)098

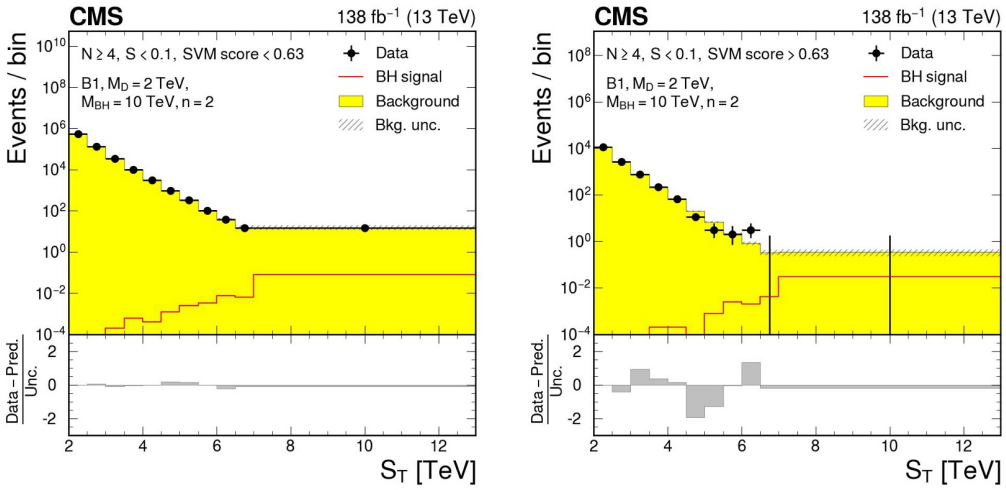


Figure 5. Post-fit S_T distributions in VR-FAIL (left) and VR-PASS (right) regions in data. The gray hatched areas include both statistical and systematic uncertainties in the background prediction (yellow histogram). The red line corresponds to the signal model B1, with $M_D = 2\,\text{TeV}$, $M_{BH} = 10\,\text{TeV}$, and $n = 2$. The lower panels show the difference between observed data and the background prediction, normalized by the total uncertainty.

8 Systematic uncertainties

The systematic uncertainties are incorporated as nuisance parameters and are profiled in the maximum likelihood fit.

The uncertainty in the integrated luminosity is applied as a 0.73% uncertainty affecting the signal normalization [80]. The uncertainty associated with pileup is estimated by varying the total inelastic cross section [81], which is used to compute the event weights, by one standard deviation. This variation is then applied to the signal events to match the pileup distribution observed in data. The resulting variations due to the pileup uncertainty are below 1% across all signal mass points.

The uncertainties in the jet energy corrections [61, 82, 83] are included in both background estimation methods. This leads to subdominant ($< 1\%$) uncertainties.

For the SI background estimation method, the primary sources of systematic uncertainty are associated with extrapolating the background from the CR to the SR and its normalization. The extrapolation uncertainty arises from the procedure used to model the background and it accounts for the range of possible background functions that fit the data in the fit region. The uncertainty is derived from the envelope of the highest and lowest fits obtained from the 16 test functions, which vary with multiplicity and S_T. For $S_T > 5.2\,\text{TeV}$, where the background prediction relies on an extrapolation beyond the fit region, this procedure results in a conservative uncertainty of approximately 50% in the nominal background prediction for all values of N.

An additional uncertainty is introduced to account for residual variations and possible non-invariance in the low-S_T region due to initial-state radiation. This uncertainty is assigned a baseline value of 30% and increases with S_T, reaching up to 120% in the high-S_T region.

JHEP08(2026)098

A background normalization uncertainty associated with the procedure described above accounts for variations in the low-S_T normalization region, and ranges from 0.6 to 10%, depending on multiplicity.

For the PS method, the background uncertainty has two sources: the statistical uncertainty in the background yield in the FAIL region, which varies from 1% to 100% as S_T increases, and the statistical uncertainty in $R_{P/F}$, which varies from 1% to 10% depending on S_T.

Both methods are statistically limited.

9 Results

The results of the search are extracted by performing a simultaneous maximum likelihood fit with the CMS statistical analysis tool Combine [84], which is based on the RooFit [85] and RooStats [86] frameworks. They are interpreted in terms of model-independent limits on BSM physics in energetic, multiparticle final states, and as model-dependent limits for a set of semiclassical BH and SB scenarios, as well as for EW sphalerons.

Limits are set using the CL_s method [87–89] with log-normal priors in the likelihood to constrain the nuisance parameters near their best fit values. We do not use the asymptotic approximation of the CL_s method [90], as most models in the search region have very low expected background, a condition for which the asymptotic approximation is known to overestimate the search sensitivity.

9.1 Model-independent results

Figure 6 shows the S_T distribution in the SI-SR in data along with the background prediction and its uncertainty. No significant deviation in data compared to the expected SM background is observed.

Model-independent 95% confidence level (CL) limits on the signal cross section for $S_T > S_T^{min}$ times acceptance (A) are derived for a generic signal producing events above a threshold S_T^{min}. These limits do not rely on assumptions about the signal model's properties or production mechanism. Acceptance is defined with respect to a fiducial phase space corresponding to the full event and object selection used in the analysis. This includes the requirements on reconstructed objects, event multiplicity, and the sphericity selection $S > 0.1$. For sphaleron signal models, the acceptance is typically high, ranging from 89% to 93%. For microscopic black hole signals, the acceptance depends strongly on the mass point and model parameters. In the case of the B1 model, the acceptance varies between approximately 50% and 90% across the considered parameter space. The observed number of events in the SI-SR sample is compared to the expected number of background events coming from the extrapolation of the fitted function, allowing for a limit to be set on any excess of events that could indicate the presence of a signal.

Figure 7 (left) shows the expected median limits, with 68% and 95% quantile bands, and observed limits for $N \geq 4$. We show the observed limits for different object multiplicity thresholds in figure 7 (right) as functions of the S_T threshold. The observed limits show an improvement of about a factor of 4 over the previous CMS analysis [21]. The gain comes from both the increased integrated luminosity and the enhanced background rejection provided by the sphericity selection.

JHEP08(2026)098

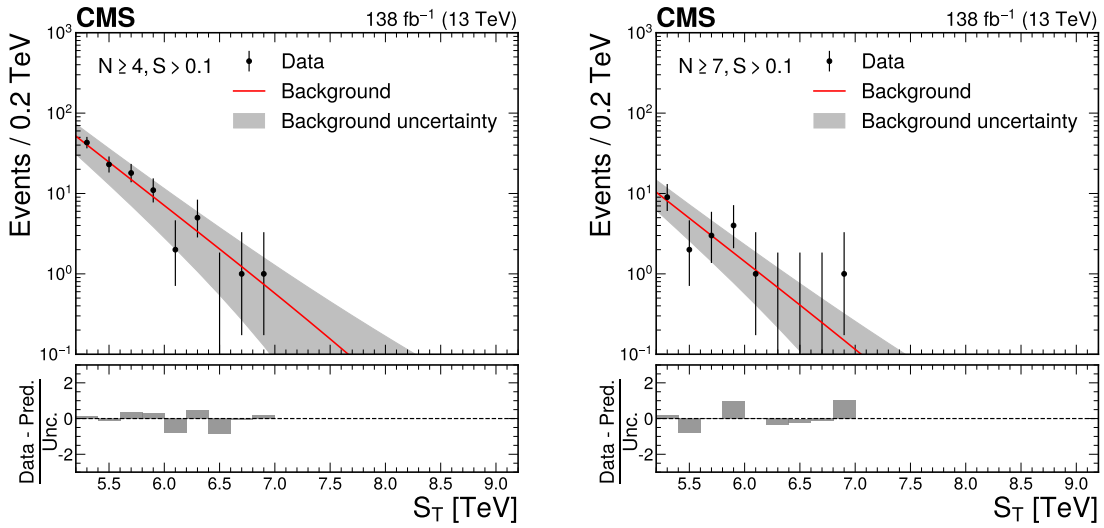


Figure 6. The S_T distribution in the $N \geq 4$ (left) and $N \geq 7$ (right) SI-SR in data, indicated by the black dots, along with the background prediction and its uncertainty represented by the red line and gray band, respectively. The error bars on the data points correspond to Poisson confidence intervals associated with the observed event counts. Lower panel as in figure 4.

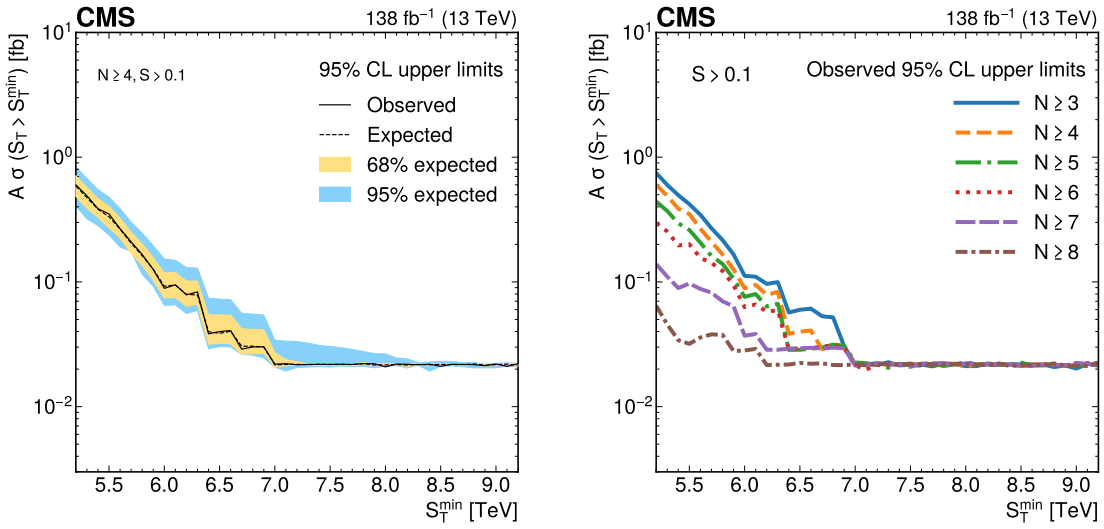


Figure 7. Expected and observed model-independent 95% CL upper limits on the cross section times acceptance for multiplicity $N \geq 4$, where the inner (outer) band represents the 68% (95%) quantile of the expected limit (left), and the observed limits with different minimum object multiplicity requirements (right).

JHEP08(2026)098

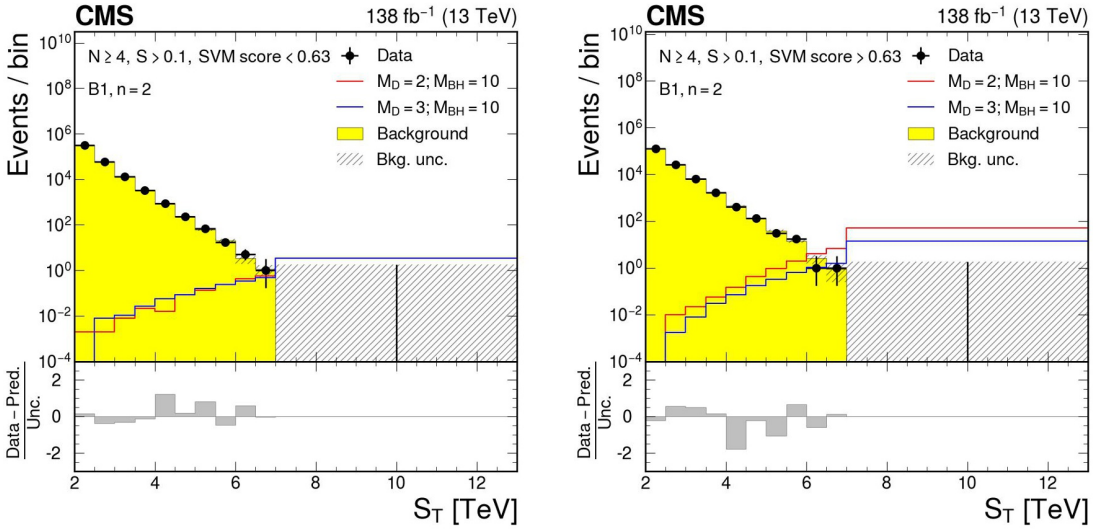


Figure 8. Post-fit S_T distributions in the FAIL (left) and PASS (right) regions in data. The gray shaded area includes both statistical and systematic uncertainties in the background prediction (yellow histogram) while the red and blue lines are B1 signal examples, as noted in the legends. Lower panel as in figure 5.

9.2 Model-dependent results

Model-dependent results are derived using the PS method for background estimation, with limits set using the S_T distribution in the SR, defined by $N \geq 4$, $S > 0.1$, and SVM score > 0.63. The background prediction and observed data for the PS method are shown in figure 8, together with the B1 model at $n = 2$ with $M_D = 2$ TeV, $M_{BH} = 10$ TeV (red) and with $M_D = 3$ TeV, $M_{BH} = 10$ TeV (blue) as examples of expected signal distributions. No significant deviation in data compared to the expected SM background is observed.

In figure 9, we compare the observed upper limits on the signal cross section to the predicted cross section. In the B1 model with $n = 2$, values of M_{BH} below 11.0 TeV are excluded for $M_D = 2$ TeV, and values below 10.4 TeV are excluded for $M_D = 4$ TeV.

The observed limit lies below the median expected limit at lower M_{BH} values because the observed yield in the PASS region around 4 TeV in S_T, visible in figure 8, is below the predicted background. While this bin contributes negligibly to the limits at high M_{BH}, signal models with lower threshold masses populate this region of S_T. The 68% and 95% expected uncertainty bands narrow with increasing M_{BH} as the background prediction becomes very small causing the expected limits to approach the background-free regime where the exclusion is determined primarily by the signal yield required for a 95% CL exclusion. However, the bands retain finite width across the full M_{BH} range.

Figure 10 summarizes results for excluded masses as a function of M_D for a variety of BH models, and as functions of the number of extra dimensions n. The excluded M_{BH}^{min} decreases with increasing M_D and increases with n, as expected from the corresponding behavior of the BH production cross section in the ADD framework. Rotating BH scenarios with full evaporation (B2, C1, C2) yield the strongest limits, while models with energy and

JHEP08(2026)098

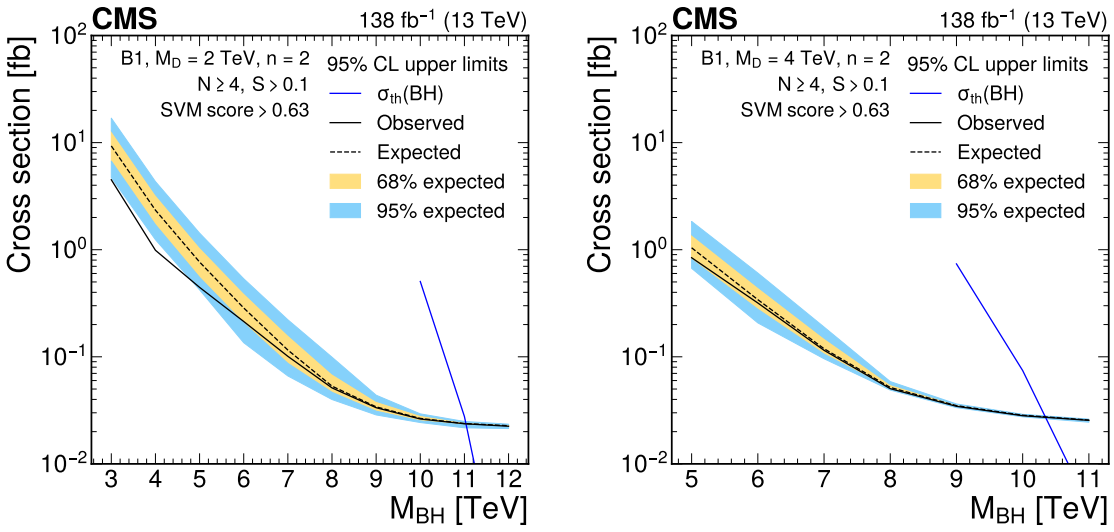


Figure 9. Expected and observed 95% CL upper limits on the cross section for a semiclassical nonrotating BH model (B1) with $n = 2$ and $M_D = 2\,\text{TeV}$ (left) or $M_D = 4\,\text{TeV}$ (right), as a function of M_{BH}. The blue curves represent the theoretical cross section values. The inner (outer) band represents the 68% (95%) quantile of the expected limit.

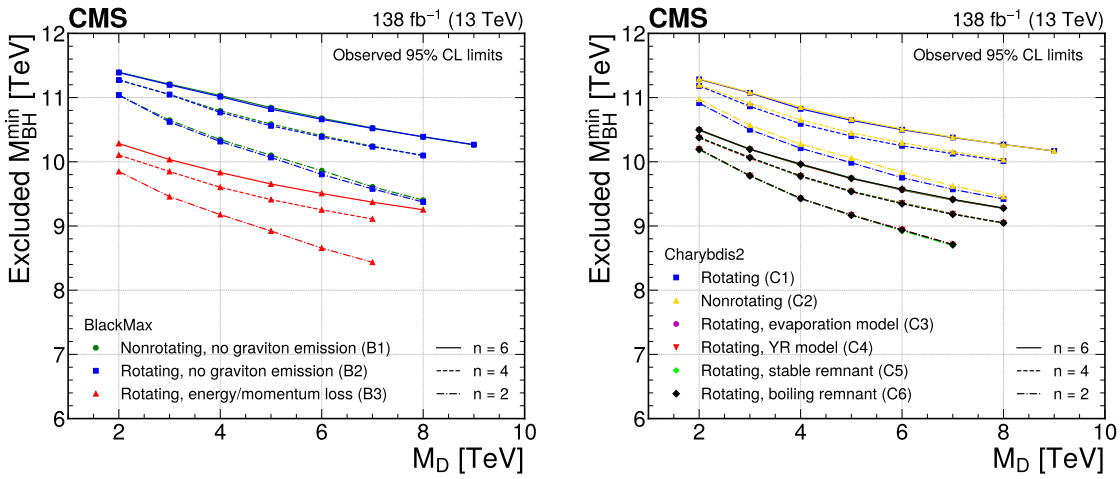


Figure 10. Excluded M_{BH}^{min} values as functions of M_D and n for a variety of BlackMax (left) and Charybdis2 (right) BH models.

momentum loss due to graviton emission (B3) or with the remnant formation (C5, C6) give weaker exclusions due to reduced visible final-state energy. Overall, M_{BH}^{min} values between approximately 9 and 11.5 TeV are excluded at 95% CL across the considered parameter space.

Taking the B1 model with $M_D = 4\,\text{TeV}$ and $n = 4$ as an example, the excluded BH mass value is extended by about 1.4 TeV with respect to the previous CMS search, where 20% of the improvement is a result of increased integrated luminosity, 20% is because of enhanced selections resulting in better signal-to-background discrimination, and 60% comes from updating PDFs from MSTW2008LO to the recent NNPDF3.1 set. This dominant

JHEP08(2026)098

PDF-driven gain is expected, as the sensitivity of the analysis is governed by events probing large parton momentum fractions, where updated PDF parameterizations lead to sizable changes in the predicted signal yield.

An alternative interpretation of these results is obtained by establishing the maximum allowed number of extra dimensions as a function of the fundamental Planck scale mass M_{D} and the minimum black hole mass $M_{\mathrm{BH}}^{\mathrm{min}}$ for different BH models. Upper limits on the number of extra dimensions n^{max} are derived as the value of n at the intersection between the experimental limit curves and the theoretical cross sections, floored to the nearest integer. This limit is well-defined because the theoretical cross section is a monotonically increasing function of n. When no intersection is found within the studied range ($n \in [2, 6]$), the result is reported as $n^{\mathrm{max}} > 6$ if the experimental limit lies above all theoretical cross sections, indicating that the exclusion does not reach $n = 6$, or as $n^{\mathrm{max}} < 2$ if it lies below, indicating that the exclusion reaches beyond $n = 2$.

At 95% CL, more than two extra dimensions are excluded under different assumptions of M_{D} and $M_{\mathrm{BH}}^{\mathrm{min}}$ for the majority of the models considered. A systematic scan over both M_{D} and $M_{\mathrm{BH}}^{\mathrm{min}}$ values is performed and the resulting parameter combinations that exclude a given number of extra dimensions are presented in table 1. For example, for models B1 and B2, the combinations $M_{\mathrm{D}} \in (2-8)\,\mathrm{TeV}$ with $M_{\mathrm{BH}}^{\mathrm{min}} \in (3, 9)\,\mathrm{TeV}$, $(2-5)\,\mathrm{TeV}$ with $M_{\mathrm{BH}}^{\mathrm{min}} = 10\,\mathrm{TeV}$, and $M_{\mathrm{D}} = 2\,\mathrm{TeV}$ with $M_{\mathrm{BH}}^{\mathrm{min}} = 11\,\mathrm{TeV}$ all yield $n^{\mathrm{max}} < 2$, i.e., the allowed number of extra dimensions are zero or one. The last row shows the combinations, typically the highest $M_{\mathrm{BH}}^{\mathrm{min}}$ with high M_{D}, when we cannot claim any exclusions. Combinations with $M_{\mathrm{BH}}^{\mathrm{min}} < M_{\mathrm{D}}$ are unphysical and not considered. A result of $n_{\mathrm{max}} < 2$ implies that, for the corresponding $(M_{\mathrm{D}}, M_{\mathrm{BH}}^{\mathrm{min}})$ combination and generator, black hole production is excluded for all values of n that are viable in the ADD model.

The upper limits on the SB production cross sections as functions of the SB mass are set for different M_{S} and g_{S} values. An example for $M_{\mathrm{S}} = 3.5\,\mathrm{TeV}$ and $g_{\mathrm{S}} = 0.2$ is shown in figure 11 (left). The excluded masses of the SB as functions of M_{S} at different g_{S} values are summarized in figure 11 (right).

For the sphaleron signal, a limit on the cross section can be converted into a limit on the pre-exponential factor, defined in section 3. Following the method in ref. [17], we calculate the limits on the pre-exponential factor for five scanned E_{sph} values: 8.5, 8.75, 9, 9.25, 9.5 TeV, under the assumptions of $p(N_{\mathrm{CS}}) = 0$, 0.5, and 1. The observed and expected 95% CL upper limits on the pre-exponential factor as functions of E_{sph} are shown in figure 12. The observed (expected) upper limit for the nominal $E_{\mathrm{sph}} = 9\,\mathrm{TeV}$ and $p(N_{\mathrm{CS}}) = 0.5$ is 0.0034 (0.0035), which is approximately 6.2 (3.4) times more stringent than the previous best limit of 0.021 (0.012) from CMS [21].

10 Summary

A dedicated search for black holes, string balls, and sphalerons produced in proton-proton collisions at $\sqrt{s} = 13\,\mathrm{TeV}$ using data collected with the CMS detector has been presented.

No excesses above the standard model background predictions are observed. We set 95% confidence level (CL) model-independent limits on cross section of hypothetical signals characterized by a large multiplicity of energetic jets, leptons, and photons. The model-

JHEP08(2026)098

(M_D [TeV], M_{BH}^{min} [TeV])					n^{max}
B1–B2	B3	C1	C2	C3–C6	
(2–8, 3–9) (2–5, 10) (2, 11)	(2–7, 3–9) (2–4, 9) (2, 11)	(2–8, 3–9) (2–4, 10)	(2–8, 3–9) (2–5, 10)	(2–7, 3–9) (2–5, 9) (2, 10)	<2
(6,10) (7, 10)	(5–6,9) (2, 10)	(5–6,10) (2, 11)	(6,10) (2, 11)	(6–7,9)	2
(8,10) (3, 11)	(7,9)	(7–8,10)	(7–8,10)	(8,9) (3,10)	3
(9,10)	(8,9)	(9,10)	(9,10) (3,11)	—	4
(4,11)	(3,10)	(3,11)	—	—	5
(5–9,11)	(4–9,10) (2–9,11)	(4–9,11)	(4–9,11)	(4–9,10) (2–9,11)	>6

Table 1. Parameter combinations of the fundamental Planck scale M_D and minimum black hole mass M_{BH}^{min} (both in TeV) that exclude a given number of extra dimensions n^{max}, for BH models generated with BlackMax and Charybdis2. Each row collects all (M_D, M_{BH}^{min}) pairs yielding the same exclusion level. Combinations with $M_{BH}^{min} < M_D$ are unphysical and not considered. The first row indicates the pairs that are excluded for any number of extra dimensions in the ADD model, while the last row shows the parameters where no exclusion could be made in this analysis.

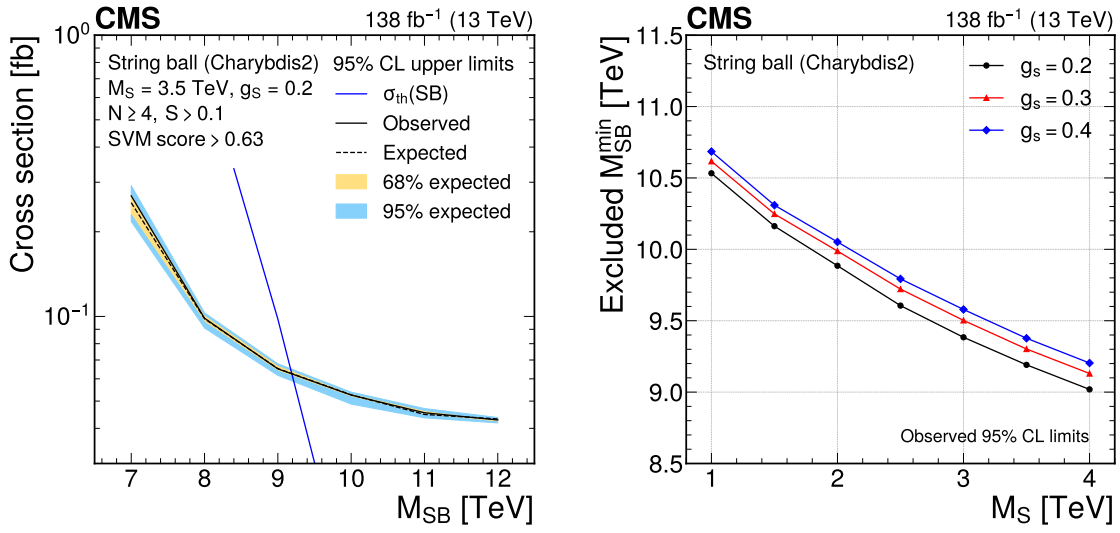


Figure 11. Expected and observed 95% CL upper limits for SB models with $M_S = 3.5$ TeV and $g_S = 0.2$ (left) and excluded SB mass values as functions of M_S at $g_S = 0.2, 0.3$, and 0.4 (right). The inner (outer) band represents the 68% (95%) quantile of the expected limit.

JHEP08(2026)098

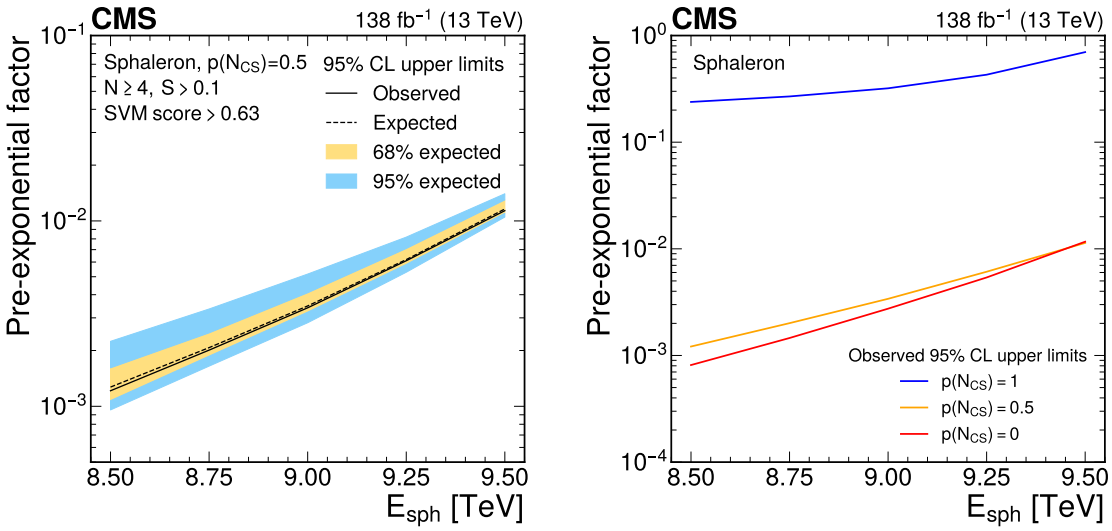


Figure 12. Expected and observed 95% CL upper limits on the pre-exponential factor for the sphaleron model with $p(N_{CS}) = 0.5$ (left), and observed limits with $p(N_{CS}) = 0$, 0.5, and 1 (right). The inner (outer) band (left) represents the 68% (95%) quantiles of the expected limit.

independent results demonstrate approximately a factor of four improvement in the cross section limit compared to the previous CMS analysis. The model-dependent results exclude at 95% CL semiclassical black holes and string balls with masses below 8.4–11.4 TeV and 9.0–10.7 TeV, respectively, depending on the model and the number of extra dimensions. This extends the exclusion reach by 1–1.6 TeV and 1.3–1.9 TeV, respectively. The observed (expected) upper limit on the sphaleron pre-exponential factor for the nominal electroweak sphaleron transition energy of 9 TeV is 0.0034 (0.0035) at 95% CL, which is strengthened by a factor of 6.2 (3.4) compared to the previous best limit of 0.021 (0.012) from CMS [21]. These are the most stringent limits on the sphaleron pre-exponential factor to date. A significant improvement in the model-dependent study over previous results comes from an improved understanding of parton distribution functions. Additional significant gains can be traced to both the increased integrated luminosity, and the enhanced background rejection provided by the sphericity and phase space distance event selection requirements.

Acknowledgments

We congratulate our colleagues in the CERN accelerator departments for the excellent performance of the LHC and thank the technical and administrative staffs at CERN and at other CMS institutes for their contributions to the success of the CMS effort. In addition, we gratefully acknowledge the computing centers and personnel of the Worldwide LHC Computing Grid and other centers for delivering so effectively the computing infrastructure essential to our analyses. Finally, we acknowledge the enduring support for the construction and operation of the LHC, the CMS detector, and the supporting computing infrastructure provided by the following funding agencies: SC (Armenia), BMBWF and FWF (Austria); FNRS and FWO (Belgium); CNPq, CAPES, FAPERJ, FAPERGS, and FAPESP (Brazil);

JHEP08(2026)098

MES and BNSF (Bulgaria); CERN; CAS, MoST, and NSFC (China); MINCIENCIAS (Colombia); MSES and CSF (Croatia); RIF (Cyprus); SENESCYT (Ecuador); ERC PRG and PSG, TARISTU24-TK10 and MoER TK202 (Estonia); Academy of Finland, MEC, and HIP (Finland); CEA and CNRS/IN2P3 (France); SRNSF (Georgia); BMFTR, DFG, and HGF (Germany); GSRI (Greece); MATE and NKFIH (Hungary); DAE and DST (India); IPM (Iran); SFI (Ireland); INFN (Italy); MSIT and NRF (Republic of Korea); MES (Latvia); LMTLT (Lithuania); MOE and UM (Malaysia); BUAP, CINVESTAV, CONACYT, LNS, SEP, and UASLP-FAI (Mexico); MOS (Montenegro); MBIE (New Zealand); PAEC (Pakistan); MSHE, NSC, and NAWA (Poland); FCT (Portugal); MESTD (Serbia); MICIU/AEI and PCTI (Spain); MOSTR (Sri Lanka); Swiss Funding Agencies (Switzerland); MST (Taipei); MHESI (Thailand); TUBITAK and TENMAK (Türkiye); NASU (Ukraine); STFC (United Kingdom); DOE and NSF (U.S.A.).

Individuals have received support from the Marie-Curie program and the European Research Council and Horizon 2020 Grant, contract Nos. 675440, 724704, 752730, 758316, 765710, 824093, 101115353, 101002207, 101001205, and COST Action CA16108 (European Union); the Leventis Foundation; the Alfred P. Sloan Foundation; the Alexander von Humboldt Foundation; the Science Committee, project no. 22rl-037 (Armenia); the Fonds pour la Formation à la Recherche dans l'Industrie et dans l'Agriculture (FRIA) and Fonds voor Wetenschappelijk Onderzoek contract No. 1228724N (Belgium); the Beijing Municipal Science & Technology Commission, No. Z191100007219010, the Fundamental Research Funds for the Central Universities, the Ministry of Science and Technology of China under Grant No. 2023YFA1605804, the Natural Science Foundation of China under Grant No. 12535004, and USTC Research Funds of the Double First-Class Initiative No. YD2030002017 (China); the Ministry of Education, Youth and Sports (MEYS) of the Czech Republic; the Shota Rustaveli National Science Foundation, grant FR-22-985 (Georgia); the Deutsche Forschungsgemeinschaft (DFG), among others, under Germany's Excellence Strategy – EXC 2121 "Quantum Universe" – 390833306, and under project number 400140256 – GRK2497; the Hellenic Foundation for Research and Innovation (HFRI), Project Number 2288 (Greece); the Hungarian Academy of Sciences, the New National Excellence Program – ÚNKP, the NKFIH research grants K 131991, K 138136, K 143460, K 143477, K 147557, K 146913, K 146914, K 147048, TKP2021-NKTA-64, and 2025-1.1.5-NEMZ_KI-2025-00004, and MATE KKP and KKPCs Research Excellence and Flagship Research Groups grants (Hungary); the Council of Science and Industrial Research, India; ICSC – National Research Center for High Performance Computing, Big Data and Quantum Computing, FAIR – Future Artificial Intelligence Research, and CUP I53D23001070006 (Mission 4 Component 1), funded by the NextGenerationEU program, the Italian Ministry of University and Research (MUR) under Bando PRIN 2022 – CUP I53C24002390006, PRIN PRIMULA 2022RBYK7T (Italy); the Latvian Council of Science; the Ministry of Science and Higher Education, project no. 2022/WK/14, and the National Science Center, contracts Opus 2021/41/B/ST2/01369, 2021/43/B/ST2/01552, 2023/49/B/ST2/03273, and the NAWA contract BPN/PPO/2021/1/00011 (Poland); the Fundação para a Ciência e a Tecnologia (Portugal); the National Priorities Research Program by Qatar National Research Fund; MICIU/AEI/10.13039/501100011033, ERDF/EU, "European Union NextGenerationEU/PRTR", projects PID2022-142604OB-C21, PID2022-139519OB-

JHEP08(2026)098

C21, PID2023-147706NB-I00, PID2023-148896NB-I00, PID2023-146983NB-I00, PID2023-147115NB-I00, PID2023-148418NB-C41, PID2023-148418NB-C42, PID2023-148418NB-C43, PID2023-148418NB-C44, PID2024-158190NB-C22, RYC2021-033305-I, RYC2024-048719-I, CNS2023-144781, CNS2024-154769 and Plan de Ciencia, Tecnología e Innovación de Asturias, Spain; the Chulalongkorn Academic into Its 2nd Century Project Advancement Project, the National Science, Research and Innovation Fund program IND_FF_68_369_2300_097, and the Program Management Unit for Human Resources & Institutional Development, Research and Innovation, grant B39G680009 (Thailand); the Eric & Wendy Schmidt Fund for Strategic Innovation through the CERN Next Generation Triggers project under grant agreement number SIF-2023-004; the Kavli Foundation; the Nvidia Corporation; the SuperMicro Corporation; the Welch Foundation, contract C-1845; and the Weston Havens Foundation (U.S.A.).

Data Availability Statement. Release and preservation of data used by the CMS Collaboration as the basis for publications is guided by the CMS data preservation, re-use and open access policy.

Code Availability Statement. The CMS core software is publicly available on GitHub.

Open Access. This article is distributed under the terms of the Creative Commons Attribution License (CC-BY4.0), which permits any use, distribution and reproduction in any medium, provided the original author(s) and source are credited.

References

[1] I. Antoniadis, N. Arkani-Hamed, S. Dimopoulos and G.R. Dvali, *New dimensions at a millimeter to a Fermi and superstrings at a TeV*, *Phys. Lett. B* **436** (1998) 257 [hep-ph/9804398] [INSPIRE].

[2] N. Arkani-Hamed, S. Dimopoulos and G.R. Dvali, *The hierarchy problem and new dimensions at a millimeter*, *Phys. Lett. B* **429** (1998) 263 [hep-ph/9803315] [INSPIRE].

[3] N. Arkani-Hamed, S. Dimopoulos and G.R. Dvali, *Phenomenology, astrophysics and cosmology of theories with submillimeter dimensions and TeV scale quantum gravity*, *Phys. Rev. D* **59** (1999) 086004 [hep-ph/9807344] [INSPIRE].

[4] L. Randall and R. Sundrum, *An alternative to compactification*, *Phys. Rev. Lett.* **83** (1999) 4690 [hep-th/9906064] [INSPIRE].

[5] L. Randall and R. Sundrum, *A large mass hierarchy from a small extra dimension*, *Phys. Rev. Lett.* **83** (1999) 3370 [hep-ph/9905221] [INSPIRE].

[6] S. Dimopoulos and G.L. Landsberg, *Black holes at the LHC*, *Phys. Rev. Lett.* **87** (2001) 161602 [hep-ph/0106295] [INSPIRE].

[7] P.C. Argyres, S. Dimopoulos and J. March-Russell, *Black holes and submillimeter dimensions*, *Phys. Lett. B* **441** (1998) 96 [hep-th/9808138] [INSPIRE].

[8] S.B. Giddings and S.D. Thomas, *High-energy colliders as black hole factories: The end of short distance physics*, *Phys. Rev. D* **65** (2002) 056010 [hep-ph/0106219] [INSPIRE].

[9] S.W. Hawking, *Particle Creation by Black Holes*, *Commun. Math. Phys.* **43** (1975) 199 [*Erratum ibid.* **46** (1976) 206] [INSPIRE].

[10] P. Meade and L. Randall, *Black Holes and Quantum Gravity at the LHC*, *JHEP* **05** (2008) 003 [arXiv:0708.3017] [INSPIRE].

JHEP08(2026)098

[11] D.M. Gingrich, *Quantum black holes with charge, colour, and spin at the LHC*, *J. Phys. G* **37** (2010) 105008 [arXiv:0912.0826] [INSPIRE].

[12] X. Calmet, W. Gong and S.D.H. Hsu, *Colorful quantum black holes at the LHC*, *Phys. Lett. B* **668** (2008) 20 [arXiv:0806.4605] [INSPIRE].

[13] S. Dimopoulos and R. Emparan, *String balls at the LHC and beyond*, *Phys. Lett. B* **526** (2002) 393 [hep-ph/0108060] [INSPIRE].

[14] G. 't Hooft, *Symmetry Breaking Through Bell-Jackiw Anomalies*, *Phys. Rev. Lett.* **37** (1976) 8 [INSPIRE].

[15] F.R. Klinkhamer and N.S. Manton, *A Saddle Point Solution in the Weinberg-Salam Theory*, *Phys. Rev. D* **30** (1984) 2212 [INSPIRE].

[16] S.-H.H. Tye and S.S.C. Wong, *Bloch Wave Function for the Periodic Sphaleron Potential and Unsuppressed Baryon and Lepton Number Violating Processes*, *Phys. Rev. D* **92** (2015) 045005 [arXiv:1505.03690] [INSPIRE].

[17] J. Ellis and K. Sakurai, *Search for Sphalerons in Proton-Proton Collisions*, *JHEP* **04** (2016) 086 [arXiv:1601.03654] [INSPIRE].

[18] A. Papaefstathiou, S. Plätzer and K. Sakurai, *On the phenomenology of sphaleron-induced processes at the LHC and beyond*, *JHEP* **12** (2019) 017 [arXiv:1910.04761] [INSPIRE].

[19] ATLAS collaboration, *Search for strong gravity in multijet final states produced in pp collisions at $\sqrt{s} = 13$ TeV using the ATLAS detector at the LHC*, *JHEP* **03** (2016) 026 [arXiv:1512.02586] [INSPIRE].

[20] ATLAS collaboration, *Search for quantum black hole production in lepton+jet final states using proton-proton collisions at $\sqrt{s} = 13$ TeV with the ATLAS detector*, *Phys. Rev. D* **109** (2024) 032010 [arXiv:2307.14967] [INSPIRE].

[21] CMS collaboration, *Search for black holes and sphalerons in high-multiplicity final states in proton-proton collisions at $\sqrt{s} = 13$ TeV*, *JHEP* **11** (2018) 042 [arXiv:1805.06013] [INSPIRE].

[22] CMS collaboration, *Search for Microscopic Black Hole Signatures at the Large Hadron Collider*, *Phys. Lett. B* **697** (2011) 434 [arXiv:1012.3375] [INSPIRE].

[23] CMS collaboration, *Search for Microscopic Black Holes in pp Collisions at $\sqrt{s} = 7$ TeV*, *JHEP* **04** (2012) 061 [arXiv:1202.6396] [INSPIRE].

[24] CMS collaboration, *Search for Microscopic Black Holes in pp Collisions at $\sqrt{s} = 8$ TeV*, *JHEP* **07** (2013) 178 [arXiv:1303.5338] [INSPIRE].

[25] CMS collaboration, *Search for black holes in high-multiplicity final states in proton-proton collisions at $\sqrt{s} = 13$ TeV*, *Phys. Lett. B* **774** (2017) 279 [arXiv:1705.01403] [INSPIRE].

[26] HEPData record for this analysis, (2025) DOI:10.17182/hepdata.165871.

[27] CMS collaboration, *The CMS Experiment at the CERN LHC*, 2008 *JINST* **3** S08004 [arXiv:1003.4038] [INSPIRE].

[28] CMS collaboration, *Development of the CMS detector for the CERN LHC Run 3*, 2024 *JINST* **19** P05064 [arXiv:2309.05466] [INSPIRE].

[29] CMS collaboration, *Description and Performance of Track and Primary-Vertex Reconstruction with the CMS Tracker*, 2014 *JINST* **9** P10009 [arXiv:1405.6569] [INSPIRE].

[30] CMS Tracker Group collaboration, *The CMS Phase-1 Pixel Detector Upgrade*, 2021 *JINST* **16** P02027 [arXiv:2012.14304] [INSPIRE].

[31] CMS collaboration, *Track impact parameter resolution for the full pseudo rapidity coverage in the 2017 dataset with the CMS Phase-1 Pixel detector*, CMS-DP-2020-049 (2020).

[32] CMS collaboration, *2017 tracking performance plots*, CMS-DP-2017-015 (2017).

JHEP08(2026)098

[33] CMS collaboration, *Performance of the CMS Level-1 trigger in proton-proton collisions at* $\sqrt{s} = 13$ *TeV*, 2020 *JINST* **15** P10017 [arXiv:2006.10165] [INSPIRE].

[34] CMS collaboration, *The CMS trigger system*, 2017 *JINST* **12** P01020 [arXiv:1609.02366] [INSPIRE].

[35] CMS collaboration, *Performance of the CMS high-level trigger during LHC Run 2*, 2024 *JINST* **19** P11021 [arXiv:2410.17038] [INSPIRE].

[36] D.-C. Dai et al., *BlackMax: A black-hole event generator with rotation, recoil, split branes, and brane tension*, *Phys. Rev. D* **77** (2008) 076007 [arXiv:0711.3012] [INSPIRE].

[37] C.M. Harris, P. Richardson and B.R. Webber, *CHARYBDIS: A black hole event generator*, *JHEP* **08** (2003) 033 [hep-ph/0307305] [INSPIRE].

[38] J.A. Frost et al., *Phenomenology of Production and Decay of Spinning Extra-Dimensional Black Holes at Hadron Colliders*, *JHEP* **10** (2009) 014 [arXiv:0904.0979] [INSPIRE].

[39] C. Bravo and J. Hauser, *BaryoGEN, a Monte Carlo Generator for Sphaleron-Like Transitions in Proton-Proton Collisions*, *JHEP* **11** (2018) 041 [arXiv:1805.02786] [INSPIRE].

[40] R. Frederix et al., *The automation of next-to-leading order electroweak calculations*, *JHEP* **11** (2018) 085 [*Erratum ibid.* **11** (2021) 085] [arXiv:1804.10017] [INSPIRE].

[41] J. Alwall et al., *Comparative study of various algorithms for the merging of parton showers and matrix elements in hadronic collisions*, *Eur. Phys. J. C* **53** (2008) 473 [arXiv:0706.2569] [INSPIRE].

[42] S. Creek, O. Efthimiou, P. Kanti and K. Tamvakis, *Greybody factors for brane scalar fields in a rotating black-hole background*, *Phys. Rev. D* **75** (2007) 084043 [hep-th/0701288] [INSPIRE].

[43] S. Creek, O. Efthimiou, P. Kanti and K. Tamvakis, *Scalar Emission in the Bulk in a Rotating Black Hole Background*, *Phys. Lett. B* **656** (2007) 102 [arXiv:0709.0241] [INSPIRE].

[44] H. Yoshino and V.S. Rychkov, *Improved analysis of black hole formation in high-energy particle collisions*, *Phys. Rev. D* **71** (2005) 104028 [*Erratum ibid.* **77** (2008) 089905] [hep-th/0503171] [INSPIRE].

[45] B. Koch, M. Bleicher and S. Hossenfelder, *Black hole remnants at the LHC*, *JHEP* **10** (2005) 053 [hep-ph/0507138] [INSPIRE].

[46] H. Stoecker, *Stable TeV — Black Hole Remnants at the LHC: Discovery through Di-Jet Suppression, Mono-Jet Emission and a Supersonic Boom in the Quark-Gluon Plasma*, *Int. J. Mod. Phys. D* **16** (2007) 185 [hep-ph/0605062] [INSPIRE].

[47] F. Scardigli, *Glimpses on the micro black hole Planck phase*, *Symmetry* **12** (2020) 1519 [arXiv:0809.1832] [INSPIRE].

[48] D.M. Gingrich and K. Martell, *Study of highly-excited string states at the Large Hadron Collider*, *Phys. Rev. D* **78** (2008) 115009 [arXiv:0808.2512] [INSPIRE].

[49] CMS collaboration, *Extraction and validation of a new set of CMS PYTHIA8 tunes from underlying-event measurements*, *Eur. Phys. J. C* **80** (2020) 4 [arXiv:1903.12179] [INSPIRE].

[50] NNPDF collaboration, *Parton distributions from high-precision collider data*, *Eur. Phys. J. C* **77** (2017) 663 [arXiv:1706.00428] [INSPIRE].

[51] CMS collaboration, *Upgrades for the CMS simulation*, *J. Phys. Conf. Ser.* **608** (2015) 012056 [INSPIRE].

[52] CMS collaboration, *Particle-flow reconstruction and global event description with the CMS detector*, 2017 *JINST* **12** P10003 [arXiv:1706.04965] [INSPIRE].

[53] CMS collaboration, *Technical proposal for the Phase-II upgrade of the Compact Muon Solenoid*, CERN-LHCC-2015-010 (2015).

JHEP08(2026)098

[54] CMS collaboration, *Jet energy scale and resolution in the CMS experiment in pp collisions at 8 TeV*, 2017 *JINST* **12** P02014 [arXiv:1607.03663] [INSPIRE].

[55] CMS collaboration, *Pileup Removal Algorithms*, CMS-PAS-JME-14-001 (2014) [INSPIRE].

[56] CMS collaboration, *Jet algorithms performance in 13 TeV data*, CMS-PAS-JME-16-003 (2017) [INSPIRE].

[57] CMS collaboration, *Performance of electron reconstruction and selection with the CMS detector in proton-proton collisions at* $\sqrt{s} = 8$ *TeV*, 2015 *JINST* **10** P06005 [arXiv:1502.02701] [INSPIRE].

[58] CMS collaboration, *Electron and photon reconstruction and identification with the CMS experiment at the CERN LHC*, 2021 *JINST* **16** P05014 [arXiv:2012.06888] [INSPIRE].

[59] CMS collaboration, *Performance of CMS Muon Reconstruction in pp Collision Events at* $\sqrt{s} = 7$ *TeV*, 2012 *JINST* **7** P10002 [arXiv:1206.4071] [INSPIRE].

[60] CMS collaboration, *Performance of the CMS muon detector and muon reconstruction with proton-proton collisions at* $\sqrt{s} = 13$ *TeV*, 2018 *JINST* **13** P06015 [arXiv:1804.04528] [INSPIRE].

[61] CMS collaboration, *Performance of missing transverse momentum reconstruction in proton-proton collisions at* $\sqrt{s} = 13$ *TeV using the CMS detector*, 2019 *JINST* **14** P07004 [arXiv:1903.06078] [INSPIRE].

[62] ALEPH collaboration, *Studies of quantum chromodynamics with the ALEPH detector*, *Phys. Rept.* **294** (1998) 1 [INSPIRE].

[63] ATLAS collaboration, *Measurement of event shapes at large momentum transfer with the ATLAS detector in pp collisions at* $\sqrt{s} = 7$ *TeV*, *Eur. Phys. J. C* **72** (2012) 2211 [arXiv:1206.2135] [INSPIRE].

[64] ALICE collaboration, *Transverse sphericity of primary charged particles in minimum bias proton-proton collisions at* $\sqrt{s} = 0.9$, 2.76 *and* 7 *TeV*, *Eur. Phys. J. C* **72** (2012) 2124 [arXiv:1205.3963] [INSPIRE].

[65] P.T. Komiske, E.M. Metodiev and J. Thaler, *Metric Space of Collider Events*, *Phys. Rev. Lett.* **123** (2019) 041801 [arXiv:1902.02346] [INSPIRE].

[66] P.T. Komiske, E.M. Metodiev and J. Thaler, *The Hidden Geometry of Particle Collisions*, *JHEP* **07** (2020) 006 [arXiv:2004.04159] [INSPIRE].

[67] T. Cai, J. Cheng, K. Craig and N. Craig, *Which metric on the space of collider events?*, *Phys. Rev. D* **105** (2022) 076003 [arXiv:2111.03670] [INSPIRE].

[68] P.T. Komiske et al., *Exploring the Space of Jets with CMS Open Data*, *Phys. Rev. D* **101** (2020) 034009 [arXiv:1908.08542] [INSPIRE].

[69] C. Cesarotti and J. Thaler, *A Robust Measure of Event Isotropy at Colliders*, *JHEP* **08** (2020) 084 [arXiv:2004.06125] [INSPIRE].

[70] C. Cesarotti, M. Reece and M.J. Strassler, *The efficacy of event isotropy as an event shape observable*, *JHEP* **07** (2021) 215 [arXiv:2011.06599] [INSPIRE].

[71] L. Gouskos et al., *Optimal transport for a novel event description at hadron colliders*, *Phys. Rev. D* **108** (2023) 096003 [arXiv:2211.02029] [INSPIRE].

[72] ATLAS collaboration, *Measurements of multijet event isotropies using optimal transport with the ATLAS detector*, *JHEP* **10** (2023) 060 [arXiv:2305.16930] [INSPIRE].

[73] A.J. Larkoski and T. Melia, *Covariantizing phase space*, *Phys. Rev. D* **102** (2020) 094014 [arXiv:2008.06508] [INSPIRE].

[74] T. Cai et al., *The phase space distance between collider events*, *JHEP* **09** (2024) 054 [arXiv:2405.16698] [INSPIRE].

JHEP08(2026)098

[75] C. Cortes and V. Vapnik, *Support-vector networks*, *Mach. Learn.* **20** (1995) 273 [INSPIRE].

[76] G. Punzi, *Sensitivity of searches for new signals and its optimization*, *eConf C* **030908** (2003) MODT002 [physics/0308063] [INSPIRE].

[77] L. Corcodilos, *The 2D Alphabet background modeling method and its use in the search for an excited bottom quark*, Ph.D. thesis, Johns Hopkins U. (main), Johns Hopkins University, Johns Hopkins University, U.S.A. (2021) [INSPIRE].

[78] R.A. Fisher, *On the Interpretation of χ^2 from Contingency Tables, and the Calculation of P*, *J. Roy. Statist. Soc.* **85** (1922) 87.

[79] S. Baker and R.D. Cousins, *Clarification of the Use of Chi Square and Likelihood Functions in Fits to Histograms*, *Nucl. Instrum. Meth.* **221** (1984) 437 [INSPIRE].

[80] CMS collaboration, *Precision luminosity measurement in proton-proton collisions at $\sqrt{s} = 13$ TeV with the CMS detector*, CMS-PAS-LUM-20-001 (2025) [INSPIRE].

[81] CMS collaboration, *Measurement of the inelastic proton-proton cross section at $\sqrt{s} = 13$ TeV*, *JHEP* **07** (2018) 161 [arXiv:1802.02613] [INSPIRE].

[82] CMS collaboration, *Identification of heavy, energetic, hadronically decaying particles using machine-learning techniques*, 2020 *JINST* **15** P06005 [arXiv:2004.08262] [INSPIRE].

[83] CMS collaboration, *Pileup mitigation at CMS in 13 TeV data*, 2020 *JINST* **15** P09018 [arXiv:2003.00503] [INSPIRE].

[84] CMS collaboration, *The CMS Statistical Analysis and Combination Tool: Combine*, *Comput. Softw. Big Sci.* **8** (2024) 19 [arXiv:2404.06614] [INSPIRE].

[85] W. Verkerke and D.P. Kirkby, *The RooFit toolkit for data modeling*, *eConf C* **0303241** (2003) MOLT007 [physics/0306116] [INSPIRE].

[86] L. Moneta et al., *The RooStats Project*, *PoS* **ACAT2010** (2010) 057 [arXiv:1009.1003] [INSPIRE].

[87] T. Junk, *Confidence level computation for combining searches with small statistics*, *Nucl. Instrum. Meth. A* **434** (1999) 435 [hep-ex/9902006] [INSPIRE].

[88] A.L. Read, *Presentation of search results: The CL_s technique*, *J. Phys. G* **28** (2002) 2693 [INSPIRE].

[89] ATLAS et al. collaborations, *Procedure for the LHC Higgs boson search combination in Summer 2011*, CMS-NOTE-2011-005 (2011) [INSPIRE].

[90] G. Cowan, K. Cranmer, E. Gross and O. Vitells, *Asymptotic formulae for likelihood-based tests of new physics*, *Eur. Phys. J. C* **71** (2011) 1554 [*Erratum ibid.* **73** (2013) 2501] [arXiv:1007.1727] [INSPIRE].

JHEP08(2026)098

The CMS collaboration

A. Hayrapetyan[1], V. Makarenko[1], A. Tumasyan[1,a], W. Adam[2], L. Benato[2], T. Bergauer[2], M. Dragicevic[2], P.S. Hussain[2], M. Jeitler[2,b], N. Krammer[2], A. Li[2], D. Liko[2], M. Matthewman[2], J. Schieck[2,b], R. Schöfbeck[2,b], M. Shooshtari[2], M. Sonawane[2], W. Waltenberger[2], C.-E. Wulz[2,b], T. Janssen[3], H. Kwon[3], D. Ocampo Henao[3], T. Van Laer[3], P. Van Mechelen[3], J. Bierkens[4], N. Breugelmans[4], J. D'Hondt[4], S. Dansana[4], A. De Moor[4], M. Delcourt[4], C. Gupta[4], F. Heyen[4], Y. Hong[4], P. Kashko[4], S. Lowette[4], I. Makarenko[4], S. Tavernier[4], M. Tytgat[4,c], G.P. Van Onsem[4], S. Van Putte[4], D. Vannerom[4], B. Bilin[5], B. Clerbaux[5], A.K. Das[5], I. De Bruyn[5], G. De Lentdecker[5], H. Evard[5], L. Favart[5], P. Gianneios[5], A. Khalilzadeh[5], A. Malara[5], M.A. Shahzad[5], A. Sharma[5], L. Thomas[5], M. Vanden Bemden[5], C. Vander Velde[5], P. Vanlaer[5], F. Zhang[5], M. De Coen[6], D. Dobur[6], C. Giordano[6], G. Gokbulut[6], K. Kaspar[6], D. Kavtaradze[6], D. Marckx[6], K. Skovpen[6], A.M. Tomaru[6], N. Van Den Bossche[6], J. van der Linden[6], J. Vandenbroeck[6], H. Aarup Petersen[7], S. Bein[7], A. Benecke[7], A. Bethani[7], G. Bruno[7], A. Cappati[7], J. De Favereau De Jeneret[7], C. Delaere[7], F. Gameiro Casalinho[7], A. Giammanco[7], A.O. Guzel[7], V. Lemaitre[7], J. Lidrych[7], P. Malek[7], S. Turkcapar[7], G.A. Alves[8], M. Barroso Ferreira Filho[8], E. Coelho[8], C. Hensel[8], D. Matos Figueiredo[8], T. Menezes De Oliveira[8], C. Mora Herrera[8], P. Rebello Teles[8], M. Soeiro[8], E.J. Tonelli Manganote[8,d], A. Vilela Pereira[8], W.L. Aldá Júnior[9], H. Brandao Malbouisson[9], W. Carvalho[9], J. Chinellato[9,e], M. Costa Reis[9], E.M. Da Costa[9], G.G. Da Silveira[9,f], D. De Jesus Damiao[9], S. Fonseca De Souza[9], R. Gomes De Souza[9], S. S. Jesus[9], T. Laux Kuhn[9,f], K. Mota Amarilo[9], L. Mundim[9], H. Nogima[9], J.P. Pinheiro[9], A. Santoro[9], A. Sznajder[9], M. Thiel[9], F. Torres Da Silva De Araujo[9,g], C.A. Bernardes[10], L. Calligaris[10], F. Damas[10], T.R. Fernandez Perez Tomei[10], E.M. Gregores[10], B. Lopes Da Costa[10], I. Maietto Silverio[10], P.G. Mercadante[10], S.F. Novaes[10], Sandra S. Padula[10], V. Scheurer[10], A. Aleksandrov[11], G. Antchev[11], P. Danev[11], R. Hadjiiska[11], P. Iaydjiev[11], M. Shopova[11], G. Sultanov[11], A. Dimitrov[12], L. Litov[12], B. Pavlov[12], P. Petkov[12], A. Petrov[12], S. Keshri[13], D. Laroze[13], M. Meena[13], S. Thakur[13], W. Brooks[14], T. Cheng[15], T. Javaid[15], L. Wang[15], L. Yuan[15], Z. Hu[16], Z. Liang[16], J. Liu[16], X. Wang[16], H. Yang[16], G.M. Chen[17,h], H.S. Chen[17,h], M. Chen[17,h], Y. Chen[17], Q. Hou[17], X. Hou[17], F. Iemmi[17], C.H. Jiang[17], H. Liao[17], G. Liu[17], Z.-A. Liu[17,i], J.N. Song[17,i], S. Song[17], J. Tao[17], C. Wang[17,h], J. Wang[17], H. Zhang[17], J. Zhao[17], A. Agapitos[18], Y. Ban[18], A. Carvalho Antunes De Oliveira[18], S. Deng[18], B. Guo[18], Q. Guo[18], C. Jiang[18], A. Levin[18], C. Li[18], Q. Li[18], Y. Mao[18], S. Qian[18], S.J. Qian[18], X. Qin[18], C. Quaranta[18], X. Sun[18], D. Wang[18], J. Wang[18], M. Zhang[18], Y. Zhao[18], C. Zhou[18], S. Yang[19], Z. You[20], N. Lu[21], G. Bauer[22,j,k], Z. Cui[22,k], B. Li[22,l], H. Wang[22], K. Yi[22,m], J. Zhang[22], C. Li[23], Y. Li[24], Y. Zhou[24,n], Z. Lin[25], C. Lu[25], M. Xiao[25,o], C. Avila[26], D.A. Barbosa Trujillo[26], A. Cabrera[26], C. Florez[26], J. Fraga[26], J.A. Reyes Vega[26], C. Rendón[27], M. Rodriguez[27], A.A. Ruales Barbosa[27], J.D. Ruiz Alvarez[27], N. Godinovic[28], D. Lelas[28], A. Sculac[28], M. Kovac[29], A. Petkovic[29], T. Sculac[29], P. Bargassa[30], V. Brigljevic[30], B.K. Chitroda[30], D. Ferencek[30], K. Jakovcic[30], A. Starodumov[30], T. Susa[30], A. Attikis[31], K. Christoforou[31], S. Konstantinou[31], C. Leonidou[31], L. Paizanos[31], F. Ptochos[31], P.A. Razis[31],

JHEP08(2026)098

H. Rykaczewski[31], H. Saka[31], A. Stepennov[31], M. Finger[32,†], M. Finger Jr.[32], E. Carrera Jarrin[33], A.A. Abdelalim[34,p,q], B. El-mahdy[34,r], A. Hussein[35], H. Mohammed[35], K. Jaffel[36], M. Kadastik[36], T. Lange[36], C. Nielsen[36], J. Pata[36], M. Raidal[36], N. Seeba[36], L. Tani[36], E. Brücken[37], A. Milieva[37], K. Osterberg[37], M. Voutilainen[37], F. Garcia[38], P. Inkaew[38], K.T.S. Kallonen[38], R. Kumar Verma[38], T. Lampén[38], K. Lassila-Perini[38], B. Lehtela[38], S. Lehti[38], T. Lindén[38], N.R. Mancilla Xinto[38], M. Myllymäki[38], M.m. Rantanen[38], S. Saariokari[38], N.T. Toikka[38], J. Tuominiemi[38], N. Bin Norjoharuddeen[39], H. Kirschenmann[39], P. Luukka[39], H. Petrow[39], M. Besancon[40], F. Couderc[40], M. Dejardin[40], D. Denegri[40], P. Devouge[40], J.L. Faure[40], F. Ferri[40], P. Gaigne[40], S. Ganjour[40], P. Gras[40], F. Guilloux[40], G. Hamel de Monchenault[40], M. Kumar[40], V. Lohezic[40], Y. Maidannyk[40], J. Malcles[40], F. Orlandi[40], L. Portales[40], S. Ronchi[40], M.Ö. Sahin[40], P. Simkina[40], M. Titov[40], M. Tornago[40], R. Amella Ranz[41], F. Beaudette[41], G. Boldrini[41], P. Busson[41], C. Charlot[41], M. Chiusi[41], T.D. Cuisset[41], O. Davignon[41], A. De Wit[41], T. Debnath[41], I.T. Ehle[41], S. Ghosh[41], A. Gilbert[41], R. Granier de Cassagnac[41], L. Kalipoliti[41], M. Manoni[41], M. Nguyen[41], S. Obraztsov[41], C. Ochando[41], R. Salerno[41], J.B. Sauvan[41], Y. Sirois[41], G. Sokmen[41], Y. Song[41], L. Urda Gómez[41], A. Zabi[41], A. Zghiche[41], J.-L. Agram[42,s], J. Andrea[42], D. Bloch[42], J.-M. Brom[42], E.C. Chabert[42], C. Collard[42], G. Coulon[42], S. Falke[42], U. Goerlach[42], R. Haeberle[42], A.-C. Le Bihan[42], G. Saha[42], A. Savoy-Navarro[42,t], P. Vaucelle[42], A. Di Florio[43], B. Orzari[43], D. Amram[44], S. Beauceron[44], B. Blancon[44], G. Boudoul[44], N. Chanon[44], D. Contardo[44], P. Depasse[44], H. El Mamouni[44], J. Fay[44], E. Fillaudeau[44], S. Gascon[44], M. Gouzevitch[44], C. Greenberg[44], G. Grenier[44], B. Ille[44], E. Jourd'Huy[44], M. Lethuillier[44], B. Massoteau[44], L. Mirabito[44], A. Purohit[44], M. Vander Donckt[44], C. Verollet[44], A. Khvedelidze[45,u], I. Lomidze[45], Z. Tsamalaidze[45,u], V. Botta[46], S. Consuegra Rodríguez[46], L. Feld[46], K. Klein[46], M. Lipinski[46], P. Nattland[46], V. Oppenländer[46], A. Pauls[46], D. Pérez Adán[46], N. Röwert[46], C. Daumann[47], S. Diekmann[47], N. Eich[47], D. Eliseev[47], F. Engelke[47], J. Erdmann[47], M. Erdmann[47], B. Fischer[47], T. Hebbeker[47], K. Hoepfner[47], A. Jung[47], N. Kumar[47], M.y. Lee[47], F. Mausolf[47], M. Merschmeyer[47], A. Meyer[47], A. Pozdnyakov[47], W. Redjeb[47], H. Reithler[47], U. Sarkar[47], V. Sarkisovi[47], A. Schmidt[47], C. Seth[47], A. Sharma[47], J.L. Spah[47], V. Vaulin[47], S. Zaleski[47], M.R. Beckers[48], C. Dziwok[48], G. Flügge[48], N. Hoeflich[48], T. Kress[48], A. Nowack[48], O. Pooth[48], A. Stahl[48], A. Zotz[48], A. Abel[49], M. Aldaya Martin[49], J. Alimena[49], Y. An[49], I. Andreev[49], J. Bach[49], S. Baxter[49], H. Becerril Gonzalez[49], O. Behnke[49], A. Belvedere[49], F. Blekman[49,v], K. Borras[49,w], A. Campbell[49], S. Chatterjee[49], L.X. Coll Saravia[49], G. Eckerlin[49], D. Eckstein[49], E. Gallo[49,v], A. Geiser[49], M. Guthoff[49], A. Hinzmann[49], L. Jeppe[49], M. Kasemann[49], C. Kleinwort[49], R. Kogler[49], M. Komm[49], D. Krücker[49], W. Lange[49], D. Leyva Pernia[49], K.-Y. Lin[49], K. Lipka[49,x], W. Lohmann[49,y], J. Malvaso[49], R. Mankel[49], I.-A. Melzer-Pellmann[49], M. Mendizabal Morentin[49], A.B. Meyer[49], G. Milella[49], K. Moral Figueroa[49], A. Mussgiller[49], L.P. Nair[49], J. Niedziela[49], A. Nürnberg[49], J. Park[49], E. Ranken[49], A. Raspereza[49], D. Rastorguev[49], L. Rygaard[49], M. Scham[49,z,aa], S. Schnake[49,w], P. Schütze[49], C. Schwanenberger[49,v], D. Schwarz[49], D. Selivanova[49], K. Sharko[49], M. Shchedrolosiev[49], D. Stafford[49], M. Torkian[49],

JHEP08(2026)098

A. Ventura Barroso[49], R. Walsh[49], D. Wang[49], Q. Wang[49], K. Wichmann[49], L. Wiens[49,w], C. Wissing[49], Y. Yang[49], S. Zakharov[49], A. Zimermmane Castro Santos[49], A.R. Alves Andrade[50], M. Antonello[50], S. Bollweg[50], M. Bonanomi[50], L. Ebeling[50], K. El Morabit[50], Y. Fischer[50], M. Frahm[50], E. Garutti[50], A. Grohsjean[50], A.A. Guvenli[50], J. Haller[50], D. Hundhausen[50], G. Kasieczka[50], P. Keicher[50], R. Klanner[50], W. Korcari[50], T. Kramer[50], C.c. Kuo[50], F. Labe[50], J. Lange[50], A. Lobanov[50], J. Matthiesen[50], L. Moureaux[50], K. Nikolopoulos[50], A. Paasch[50], K.J. Pena Rodriguez[50], N. Prouvost[50], B. Raciti[50], M. Rieger[50], D. Savoiu[50], P. Schleper[50], M. Schröder[50], J. Schwandt[50], M. Sommerhalder[50], H. Stadie[50], G. Steinbrück[50], R. Ward[50], B. Wiederspan[50], M. Wolf[50], C. Yede[50], A. Brusamolino[51], E. Butz[51], Y.M. Chen[51], T. Chwalek[51], A. Dierlamm[51], G.G. Dincer[51], D. Druzhkin[51], U. Elicabuk[51], N. Faltermann[51], M. Giffels[51], A. Gottmann[51], F. Hartmann[51,ab], M. Horzela[51], F. Hummer[51], U. Husemann[51], J. Kieseler[51], M. Klute[51], J. Knolle[51], R. Kunnilan Muhammed Rafeek[51], O. Lavoryk[51], J.M. Lawhorn[51], S. Maier[51], M. Molch[51], A.A. Monsch[51], M. Mormile[51], Th. Müller[51], E. Pfeffer[51], M. Presilla[51], G. Quast[51], K. Rabbertz[51], B. Regnery[51], R. Schmieder[51], N. Shadskiy[51], I. Shvetsov[51], H.J. Simonis[51], L. Sowa[51], L. Stockmeier[51], K. Tauqeer[51], M. Toms[51], B. Topko[51], N. Trevisani[51], C. Verstege[51], T. Voigtländer[51], R.F. Von Cube[51], J. Von Den Driesch[51], C. Winter[51], R. Wolf[51], W.D. Zeuner[51], X. Zuo[51], G. Anagnostou[52], G. Daskalakis[52], A. Kyriakis[52], G. Melachroinos[53], Z. Painesis[53], I. Paraskevas[53], N. Saoulidou[53], K. Theofilatos[53], E. Tziaferi[53], E. Tzovara[53], K. Vellidis[53], I. Zisopoulos[53], T. Chatzistavrou[54], G. Karapostoli[54], K. Kousouris[54], E. Siamarkou[54], G. Tsipolitis[54], I. Evangelou[55], C. Foudas[55], P. Katsoulis[55], P. Kokkas[55], P.G. Kosmoglou Kioseoglou[55], N. Manthos[55], I. Papadopoulos[55], J. Strologas[55], C. Hajdu[56], D. Horvath[56,ac,ad], Á. Kadlecsik[56], C. Lee[56], K. Márton[56], A.J. Rádl[56,ae], F. Sikler[56], V. Veszpremi[56], M. Csanád[57], K. Farkas[57], A. Fehérkuti[57,af], M.M.A. Gadallah[57,ag], M. León Coello[57], G. Pásztor[57], G.I. Veres[57], B. Ujvari[58], G. Zilizi[58], G. Bencze[59], S. Czellar[59], J. Molnar[59], Z. Szillasi[59], T. Csorgo[60,af], F. Nemes[60,af], T. Novak[60], I. Szanyi[60,ah], S. Bahinipati[61], R. Raturi[61], S. Bansal[62], S.B. Beri[62], V. Bhatnagar[62], S. Chauhan[62], N. Dhingra[62,ai], A. Kaur[62], H. Kaur[62], M. Kaur[62], S. Kumar[62], T. Sheokand[62], J.B. Singh[62], A. Singla[62], A. Bhardwaj[63], A. Chhetri[63], B.C. Choudhary[63], A. Kumar[63], A. Kumar[63], M. Naimuddin[63], S. Phor[63], K. Ranjan[63], M.K. Saini[63], P. Palni[64], S. Acharya[65,aj], B. Gomber[65], S. Mukherjee[66], S. Bhattacharya[67], S. Das Gupta[67], S. Dutta[67], S. Dutta[67], S. Sarkar[67], M.M. Ameen[68], P.K. Behera[68], S. Chatterjee[68], G. Dash[68], A. Dattamunsi[68], P. Jana[68], P. Kalbhor[68], S. Kamble[68], J.R. Komaragiri[68,ak], T. Mishra[68], P.R. Pujahari[68], A.K. Sikdar[68], R.K. Singh[68], P. Verma[68], S. Verma[68], A. Vijay[68], B.K. Sirasva[69], L. Bhatt[70], S. Dugad[70], G.B. Mohanty[70], M. Shelake[70], P. Suryadevara[70], A. Bala[71], S. Banerjee[71], S. Barman[71,al], R.M. Chatterjee[71], M. Guchait[71], Sh. Jain[71], A. Jaiswal[71], S. Kumar[71], M. Maity[71,al], G. Majumder[71], K. Mazumdar[71], S. Parolia[71], R. Saxena[71], A. Thachayath[71], D. Maity[72,am], P. Mal[72], K. Naskar[72,am], A. Nayak[72,am], K. Pal[72], P. Sadangi[72], S.K. Swain[72], S. Varghese[72,am], D. Vats[72,am], S. Dube[73], P. Hazarika[73], B. Kansal[73], A. Laha[73], R. Sharma[73], S. Sharma[73], K.Y. Vaish[73], S. Ghosh[74], H. Bakhshiansohi[75,an], A. Jafari[75,ao], V. Sedighzadeh Dalavi[75],

JHEP08(2026)098

M. Zeinali[75,ap], S. Bashiri[76], S. Chenarani[76,aq], S.M. Etesami[76], Y. Hosseini[76], M. Khakzad[76], E. Khazaie[76], M. Mohammadi Najafabadi[76], S. Tizchang[76,ar], M. Felcini[77], M. Grunewald[77], M. Abbrescia[78a,78b], M. Barbieri[78a,78b], M. Buonsante[78a,78b], A. Colaleo[78a,78b], D. Creanza[78a,78c], N. De Filippis[78a,78c], M. De Palma[78a,78b], W. Elmetenawee[78a,78b,p], N. Ferrara[78a,78c], L. Fiore[78a], L. Generoso[78a,78b], L. Longo[78a], M. Louka[78a,78b], G. Maggi[78a,78c], M. Maggi[78a], I. Margjeka[78a], V. Mastrapasqua[78a,78b], S. My[78a,78b], F. Nenna[78a,78b], S. Nuzzo[78a,78b], A. Pellecchia[78a,78b], A. Pompili[78a,78b], G. Pugliese[78a,78c], R. Radogna[78a,78b], D. Ramos[78a], A. Ranieri[78a], L. Silvestris[78a], F.M. Simone[78a,78c], Ü. Sözbilir[78a], A. Stamerra[78a,78b], D. Troiano[78a,78b], R. Venditti[78a,78b], P. Verwilligen[78a], A. Zaza[78a,78b], G. Abbiendi[79a], D. Bonacorsi[79a,79b], P. Capiluppi[79a,79b], F.R. Cavallo[79a], M. Cuffiani[79a,79b], G.M. Dallavalle[79a], T. Diotalevi[79a,79b], F. Fabbri[79a], A. Fanfani[79a,79b], D. Fasanella[79a], P. Giacomelli[79a], C. Grandi[79a], L. Guiducci[79a,79b], S. Lo Meo[79a,as], M. Lorusso[79a,79b], L. Lunerti[79a], S. Marcellini[79a], G. Masetti[79a], F.L. Navarria[79a,79b], G. Paggi[79a,79b], A. Perrotta[79a], A.M. Rossi[79a,79b], S. Rossi Tisbeni[79a,79b], T. Rovelli[79a,79b], G.P. Siroli[79a,79b], S. Costa[80a,80b,at], A. Di Mattia[80a], A. Lapertosa[80a], R. Potenza[80a,80b], A. Tricomi[80a,80b,at], J. Altork[81a,81b], P. Assiouras[81a], G. Barbagli[81a], G. Bardelli[81a], M. Bartolini[81a,81b], A. Calandri[81a,81b], B. Camaiani[81a,81b], A. Cassese[81a], R. Ceccarelli[81a], V. Ciulli[81a,81b], C. Civinini[81a], R. D'Alessandro[81a,81b], L. Damenti[81a,81b], E. Focardi[81a,81b], T. Kello[81a], G. Latino[81a,81b], P. Lenzi[81a,81b], M. Lizzo[81a], M. Meschini[81a], S. Paoletti[81a], A. Papanastassiou[81a,81b], G. Sguazzoni[81a], L. Viliani[81a], L. Benussi[82], S. Colafranceschi[82,au], S. Meola[82,av], D. Piccolo[82], M. Alves Gallo Pereira[83a], F. Ferro[83a], E. Robutti[83a], S. Tosi[83a,83b], A. Benaglia[84a], F. Brivio[84a], V. Camagni[84a,84b], F. Cetorelli[84a,84b], F. De Guio[84a,84b], M.E. Dinardo[84a,84b], P. Dini[84a], S. Gennai[84a], R. Gerosa[84a,84b], A. Ghezzi[84a,84b], P. Govoni[84a,84b], L. Guzzi[84a], M.R. Kim[84a], G. Lavizzari[84a,84b], M.T. Lucchini[84a,84b], M. Malberti[84a], S. Malvezzi[84a], A. Massironi[84a], D. Menasce[84a], L. Moroni[84a], M. Paganoni[84a,84b], S. Palluotto[84a,84b], D. Pedrini[84a], A. Perego[84a,84b], G. Pizzati[84a,84b], T. Tabarelli de Fatis[84a,84b], S. Buontempo[85a], F. Confortini[85a,85b], C. Di Fraia[85a,85b], F. Fabozzi[85a,85c], L. Favilla[85a,85d], A.O.M. Iorio[85a,85b], L. Lista[85a,85b,aw], P. Paolucci[85a,ab], B. Rossi[85a], P. Azzi[86a], N. Bacchetta[86a,ax], L. Borella[86a], P. Bortignon[86a,86c], G. Bortolato[86a,86b], A.C.M. Bulla[86a,86c], R. Carlin[86a,86b], P. Checchia[86a], T. Dorigo[86a,ay], F. Gasparini[86a,86b], U. Gasparini[86a,86b], S. Giorgetti[86a], F. Gonella[86a], E. Lusiani[86a], M. Margoni[86a,86b], A.T. Meneguzzo[86a,86b], J. Pazzini[86a,86b], F. Primavera[86a,86b], P. Ronchese[86a,86b], R. Rossin[86a,86b], F. Simonetto[86a,86b], M. Tosi[86a,86b], A. Triossi[86a,86b], S. Ventura[86a], P. Zotto[86a,86b], A. Zucchetta[86a,86b], G. Zumerle[86a,86b], A. Braghieri[87a], M. Brunoldi[87a,87b], S. Calzaferri[87a,87b], P. Montagna[87a,87b], M. Pelliccioni[87a,87b], V. Re[87a], C. Riccardi[87a,87b], P. Salvini[87a], I. Vai[87a,87b], P. Vitulo[87a,87b], S. Ajmal[88a,88b], M.E. Ascioti[88a,88b], G.M. Bilei[88a,†], C. Carrivale[88a,88b], D. Ciangottini[88a,88b], L. Della Penna[88a,88b], L. Fanò[88a,88b], V. Mariani[88a,88b], M. Menichelli[88a], F. Moscatelli[88a,az], A. Rossi[88a,88b], A. Santocchia[88a,88b], D. Spiga[88a], T. Tedeschi[88a,88b], C. Aimè[89a,89b], C.A. Alexe[89a,89c], P. Asenov[89a,89b], P. Azzurri[89a], G. Bagliesi[89a], L. Bianchini[89a,89b], T. Boccali[89a], E. Bossini[89a], D. Bruschini[89a,89c], R. Castaldi[89a], F. Cattafesta[89a,89c], M.A. Ciocci[89a,89d], M. Cipriani[89a,89b], R. Dell'Orso[89a], S. Donato[89a,89b], R. Forti[89a,89b],

JHEP08(2026)098

A. Giassi[89a], F. Ligabue[89a,89c], A.C. Marini[89a,89b], A. Messineo[89a,89b], S. Mishra[89a], V.K. Muraleedharan Nair Bindhu[89a,89b], S. Nandan[89a], F. Palla[89a], M. Riggirello[89a,89c], A. Rizzi[89a,89b], G. Rolandi[89a,89c], S. Roy Chowdhury[89a,ba], T. Sarkar[89a], A. Scribano[89a], P. Solanki[89a,89b], P. Spagnolo[89a], F. Tenchini[89a,89b], R. Tenchini[89a], G. Tonelli[89a,89b], N. Turini[89a,89d], F. Vaselli[89a,89c], A. Venturi[89a], P.G. Verdini[89a], P. Akrap[90a,90b], C. Basile[90a,90b], S.C. Behera[90a], F. Cavallari[90a], L. Cunqueiro Mendez[90a,90b], F. De Riggi[90a,90b], D. Del Re[90a,90b], M. Del Vecchio[90a,90b], E. Di Marco[90a], M. Diemoz[90a], F. Errico[90a], L. Frosina[90a,90b], R. Gargiulo[90a,90b], B. Harikrishnan[90a,90b], F. Lombardi[90a,90b], E. Longo[90a,90b], L. Martikainen[90a,90b], G. Organtini[90a,90b], N. Palmeri[90a,90b], R. Paramatti[90a,90b], T. Pauletto[90a,90b], S. Rahatlou[90a,90b], C. Rovelli[90a], F. Santanastasio[90a,90b], L. Soffi[90a], V. Vladimirov[90a,90b], N. Amapane[91a,91b], R. Arcidiacono[91a,91c], S. Argiro[91a,91b], M. Arneodo[91a,91c,†], N. Bartosik[91a,91c], R. Bellan[91a,91b], A. Bellora[91a,91b], C. Biino[91a], C. Borca[91a,91b], N. Cartiglia[91a], M. Costa[91a,91b], R. Covarelli[91a,91b], N. Demaria[91a], E. Ferrando[91a], L. Finco[91a], M. Grippo[91a,91b], B. Kiani[91a,91b], L. Lanteri[91a,91b], F. Legger[91a], F. Luongo[91a,91b], C. Mariotti[91a], S. Maselli[91a], A. Mecca[91a,91b], L. Menzio[91a,91b], P. Meridiani[91a], E. Migliore[91a,91b], M. Monteno[91a], M.M. Obertino[91a,91b], G. Ortona[91a], L. Pacher[91a,91b], N. Pastrone[91a], M. Ruspa[91a,91c], F. Siviero[91a,91b], V. Sola[91a,91b], A. Solano[91a,91b], A. Staiano[91a], C. Tarricone[91a,91b], D. Trocino[91a], G. Umoret[91a,91b], E. Vlasov[91a,91b], R. White[91a,91b], J. Babbar[92a,92b,ba], S. Belforte[92a], V. Candelise[92a,92b], M. Casarsa[92a], F. Cossutti[92a], K. De Leo[92a], G. Della Ricca[92a,92b], R. Delli Gatti[92a,92b], C. Giraldin[92a,92b], S. Dogra[93], J. Hong[93], J. Kim[93], T. Kim[93], D. Lee[93], H. Lee[93], J. Lee[93], S.W. Lee[93], C.S. Moon[93], Y.D. Oh[93], S. Sekmen[93], B. Tae[93], Y.C. Yang[93], M.S. Kim[94], G. Bak[95], P. Gwak[95], H. Kim[95], D.H. Moon[95], J. Seo[95], E. Asilar[96], F. Carnevali[96], J. Choi[96,bb], T.J. Kim[96], Y. Ryou[96], J. Song[96], S. Ha[97], S. Han[97], B. Hong[97], J. Kim[97], K. Lee[97], K.S. Lee[97], S. Lee[97], J. Yoo[97], J. Goh[98], J. Shin[98], S. Yang[98], Y. Kang[99], H. S. Kim[99], Y. Kim[99], B. Ko[99], S. Lee[99], J. Almond[100], J.H. Bhyun[100], J. Choi[100], J. Choi[100], W. Jun[100], H. Kim[100], J. Kim[100], T. Kim[100], Y. Kim[100], Y.W. Kim[100], S. Ko[100], H. Lee[100], J. Lee[100], J. Lee[100], B.H. Oh[100], J. Shin[100], U.K. Yang[100], I. Yoon[100], W. Jang[101], D. Kim[101], S. Kim[101], J.S.H. Lee[101], Y. Lee[101], I.C. Park[101], Y. Roh[101], I.J. Watson[101], G. Cho[102], K. Hwang[102], B. Kim[102], S. Kim[102], K. Lee[102], H.D. Yoo[102], Y. Lee[103], I. Yu[103], T. Beyrouthy[104], Y. Gharbia[104], F. Alazemi[105], K. Dreimanis[106], O.M. Eberlins[106], A. Gaile[106], C. Munoz Diaz[106], D. Osite[106], G. Pikurs[106], R. Plese[106], A. Potrebko[106], M. Seidel[106], D. Sidiropoulos Kontos[106], N.R. Strautnieks[107], M. Ambrozas[108], A. Juodagalvis[108], S. Nargelas[108], S. Nayak[108], A. Rinkevicius[108], G. Tamulaitis[108], I. Yusuff[109,bc], Z. Zolkapli[109], J.F. Benitez[110], A. Castaneda Hernandez[110], A. Cota Rodriguez[110], L.E. Cuevas Picos[110], H.A. Encinas Acosta[110], L.G. Gallegos Maríñez[110], J.A. Murillo Quijada[110], L. Valencia Palomo[110], G. Ayala[111], H. Castilla-Valdez[111], H. Crotte Ledesma[111], R. Lopez-Fernandez[111], J. Mejia Guisao[111], R. Reyes-Almanza[111], A. Sánchez Hernández[111], C. Oropeza Barrera[112], M. Ramírez García[112], D.L. Ramirez Guadarrama[112], I. Bautista[113], F.E. Neri Huerta[113], I. Pedraza[113], H.A. Salazar Ibarguen[113], C. Uribe Estrada[113], I. Bubanja[114], J. Mijuskovic[114], N. Raicevic[114], P.H. Butler[115], A. Ahmad[116],

JHEP08(2026)098

M.I. Asghar[116], A. Awais[116], M.I.M. Awan[116], W.A. Khan[116], V. Avati[117], L. Forthomme[117], L. Grzanka[117], M. Malawski[117], K. Piotrzkowski[117], M. Bluj[118], M. Górski[118], M. Kazana[118], M. Szleper[118], P. Zalewski[118], K. Bunkowski[119], K. Doroba[119], A. Kalinowski[119], M. Konecki[119], J. Krolikowski[119], A. Muhammad[119], P. Fokow[120], K. Pozniak[120], W. Zabolotny[120], M. Araujo[121], D. Bastos[121], C. Beirão Da Cruz E Silva[121], A. Boletti[121], M. Bozzo[121], T. Camporesi[121], G. Da Molin[121], M. Gallinaro[121], J. Hollar[121], N. Leonardo[121], G.B. Marozzo[121], A. Petrilli[121], M. Pisano[121], J. Seixas[121], J. Varela[121], J.W. Wulff[121], P. Adzic[122], L. Markovic[122], P. Milenovic[122], V. Milosevic[122], D. Devetak[123], M. Dordevic[123], J. Milosevic[123], L. Nadderd[123], V. Rekovic[123], M. Stojanovic[123], M. Alcalde Martinez[124], J. Alcaraz Maestre[124], Cristina F. Bedoya[124], J.A. Brochero Cifuentes[124], Oliver M. Carretero[124], M. Cepeda[124], M. Cerrada[124], N. Colino[124], B. De La Cruz[124], A. Delgado Peris[124], A. Escalante Del Valle[124], D. Fernández Del Val[124], J.P. Fernández Ramos[124], J. Flix[124], M.C. Fouz[124], M. Gonzalez Hernandez[124], O. Gonzalez Lopez[124], S. Goy Lopez[124], J.M. Hernandez[124], M.I. Josa[124], J. Llorente Merino[124], C. Martin Perez[124], E. Martin Viscasillas[124], D. Moran[124], C. M. Morcillo Perez[124], Á. Navarro Tobar[124], R. Paz Herrera[124], A. Pérez-Calero Yzquierdo[124], J. Puerta Pelayo[124], I. Redondo[124], J. Vazquez Escobar[124], J.F. de Trocóniz[125], B. Alvarez Gonzalez[126], J. Ayllon Torresano[126], A. Cardini[126], J. Cuevas[126], J. Del Riego Badas[126], D. Estrada Acevedo[126], J. Fernandez Menendez[126], S. Folgueras[126], I. Gonzalez Caballero[126], P. Leguina[126], M. Obeso Menendez[126], E. Palencia Cortezon[126], J. Prado Pico[126], A. Soto Rodríguez[126], P. Vischia[126], S. Blanco Fernández[127], I.J. Cabrillo[127], A. Calderon[127], J. Duarte Campderros[127], M. Fernandez[127], G. Gomez[127], C. Lasaosa García[127], R. Lopez Ruiz[127], C. Martinez Rivero[127], P. Martinez Ruiz del Arbol[127], F. Matorras[127], P. Matorras Cuevas[127], E. Navarrete Ramos[127], J. Piedra Gomez[127], C. Quintana San Emeterio[127], L. Scodellaro[127], I. Vila[127], R. Vilar Cortabitarte[127], J.M. Vizan Garcia[127], B. Kailasapathy[128,bd], D.D.C. Wickramarathna[128], W.G.D. Dharmaratna[129,be], K. Liyanage[129], N. Perera[129], D. Abbaneo[130], C. Amendola[130], R. Ardino[130], E. Auffray[130], J. Baechler[130], D. Barney[130], J. Bendavid[130], I. Bestintzanos[130], M. Bianco[130], A. Bocci[130], L. Borgonovi[130], C. Botta[130], A. Bragagnolo[130], C.E. Brown[130], C. Caillol[130], G. Cerminara[130], P. Connor[130], K. Cormier[130], D. d'Enterria[130], A. Dabrowski[130], P. Das[130], A. David[130], A. De Roeck[130], M.M. Defranchis[130], M. Deile[130], M. Dobson[130], P.J. Fernández Manteca[130], B.A. Fontana Santos Alves[130], E. Fontanesi[130], W. Funk[130], A. Gaddi[130], S. Giani[130], D. Gigi[130], K. Gill[130], F. Glege[130], M. Glowacki[130], A. Gruber[130], J. Hegeman[130], J.K. Heikkilä[130], R. Hofsaess[130], B. Huber[130], T. James[130], P. Janot[130], O. Kaluzinska[130], O. Karacheban[130,y], G. Karathanasis[130], S. Laurila[130], P. Lecoq[130], E. Leutgeb[130], C. Lourenço[130], A.-M. Lyon[130], M. Magherini[130], L. Malgeri[130], M. Mannelli[130], A. Mehta[130], F. Meijers[130], J.A. Merlin[130], S. Mersi[130], E. Meschi[130], M. Migliorini[130], F. Monti[130], F. Moortgat[130], M. Mulders[130], M. Musich[130], I. Neutelings[130], S. Orfanelli[130], F. Pantaleo[130], M. Pari[130], G. Petrucciani[130], A. Pfeiffer[130], M. Pierini[130], M. Pitt[130], H. Qu[130], D. Rabady[130], A. Reimers[130], B. Ribeiro Lopes[130], F. Riti[130], P. Rosado[130], M. Rovere[130], H. Sakulin[130],

JHEP08(2026)098

R. Salvatico[130], S. Sanchez Cruz[130], S. Scarfi[130], M. Selvaggi[130], K. Shchelina[130], P. Silva[130], P. Sphicas[130,bf], A.G. Stahl Leiton[130], A. Steen[130], S. Summers[130], D. Treille[130], P. Tropea[130], E. Vernazza[130], J. Wanczyk[130,bg], S. Wuchterl[130], M. Zarucki[130], P. Zehetner[130], P. Zejdl[130], G. Zevi Della Porta[130], L. Caminada[131,bh], W. Erdmann[131], R. Horisberger[131], Q. Ingram[131], H.C. Kaestli[131], D. Kotlinski[131], C. Lange[131], U. Langenegger[131], A. Nigamova[131], L. Noehte[131,bh], T. Rohe[131], A. Samalan[131], T.K. Aarrestad[132], M. Backhaus[132], T. Bevilacqua[132,bh], G. Bonomelli[132], C. Cazzaniga[132], K. Datta[132], P. De Bryas Dexmiers D'Archiacchiac[132,bg], A. De Cosa[132], G. Dissertori[132], M. Dittmar[132], M. Donegà[132], F. Glessgen[132], C. Grab[132], N. Härringer[132], T.G. Harte[132], W. Lustermann[132], M. Malucchi[132], R.A. Manzoni[132], L. Marchese[132], A. Mascellani[132,bg], F. Nessi-Tedaldi[132], F. Pauss[132], B. Ristic[132], S. Rohletter[132], R. Seidita[132], J. Steggemann[132,bg], A. Tarabini[132], C.Z. Tee[132], D. Valsecchi[132], R. Wallny[132], C. Amsler[133,bi], P. Bärtschi[133], F. Bilandzija[133], M.F. Canelli[133], G. Celotto[133], V. Guglielmi[133], A. Jofrehei[133], B. Kilminster[133], T.H. Kwok[133], S. Leontsinis[133], V. Lukashenko[133], A. Macchiolo[133], F. Meng[133], M. Missiroli[133], J. Motta[133], P. Robmann[133], E. Shokr[133], F. Stäger[133], R. Tramontano[133], P. Viscone[133], D. Bhowmik[134], C.M. Kuo[134], P.K. Rout[134], S. Taj[134], P.C. Tiwari[134,ak], L. Ceard[135], K.F. Chen[135], Z.g. Chen[135], A. De Iorio[135], W.-S. Hou[135], T.h. Hsu[135], Y.w. Kao[135], S. Karmakar[135], G. Kole[135], Y.y. Li[135], R.-S. Lu[135], E. Paganis[135], X.f. Su[135], J. Thomas-Wilsker[135], L.s. Tsai[135], D. Tsionou[135], H.y. Wu[135], E. Yazgan[135], C. Asawatangtrakuldee[136], N. Srimanobhas[136], Y. Maghrbi[137], D. Agyel[138], F. Dolek[138], I. Dumanoglu[138,bj], Y. Guler[138,bk], E. Gurpinar Guler[138,bk], C. Isik[138], O. Kara[138,bl], A. Kayis Topaksu[138], Y. Komurcu[138], G. Onengut[138], K. Ozdemir[138,bm], B. Tali[138,bn], U.G. Tok[138], E. Uslan[138], I.S. Zorbakir[138], S. Sen[139], M. Yalvac[140,bo], B. Akgun[141], I.O. Atakisi[141,bp], E. Gülmez[141], M. Kaya[141,bq], O. Kaya[141,br], M.A. Sarkisla[141,bs], S. Tekten[141,bt], D. Boncukcu[142], A. Cakir[142], K. Cankocak[142,bj,bu], B. Hacisahinoglu[143], I. Hos[143,bv], B. Kaynak[143], S. Ozkorucuklu[143], O. Potok[143], H. Sert[143], C. Simsek[143], C. Zorbilmez[143], S. Cerci[144], C. Dozen[144,bw], B. Isildak[144], E. Simsek[144], D. Sunar Cerci[144], T. Yetkin[144,bw], A. Boyaryntsev[145], O. Dadazhanova[145], B. Grynyov[145], L. Levchuk[146], J.J. Brooke[147], A. Bundock[147], F. Bury[147], E. Clement[147], D. Cussans[147], D. Dharmender[147], H. Flacher[147], J. Goldstein[147], H.F. Heath[147], M.-L. Holmberg[147], L. Kreczko[147], S. Paramesvaran[147], L. Robertshaw[147], M.S. Sanjrani[147,an], J. Segal[147], V.J. Smith[147], A.H. Ball[148], K.W. Bell[148], A. Belyaev[148,bx], C. Brew[148], R.M. Brown[148], D.J.A. Cockerill[148], A. Elliot[148], K.V. Ellis[148], J. Gajownik[148], K. Harder[148], S. Harper[148], J. Linacre[148], K. Manolopoulos[148], M. Moallemi[148], D.M. Newbold[148], E. Olaiya[148], D. Petyt[148], T. Reis[148], A.R. Sahasransu[148], G. Salvi[148], T. Schuh[148], C.H. Shepherd-Themistocleous[148], I.R. Tomalin[148], K.C. Whalen[148], T. Williams[148], I. Andreou[149], R. Bainbridge[149], P. Bloch[149], O. Buchmuller[149], C.A. Carrillo Montoya[149], D. Colling[149], I. Das[149], P. Dauncey[149], G. Davies[149], M. Della Negra[149], S. Fayer[149], G. Fedi[149], G. Hall[149], H.R. Hoorani[149], A. Howard[149], G. Iles[149], C.R. Knight[149], P. Krueper[149], J. Langford[149], K.H. Law[149], J. León Holgado[149], L. Lyons[149], A.-M. Magnan[149], B. Maier[149], S. Mallios[149], A. Mastronikolis[149], M. Mieskolainen[149], J. Nash[149,by], M. Pesaresi[149], P.B. Pradeep[149], B.C. Radburn-Smith[149], A. Richards[149],

JHEP08(2026)098

A. Rose[149], L. Russell[149], K. Savva[149], R. Schmitz[149], C. Seez[149], R. Shukla[149], A. Tapper[149], K. Uchida[149], G.P. Uttley[149], T. Virdee[149,ab], M. Vojinovic[149], N. Wardle[149], D. Winterbottom[149], J. Xiao[149], J.E. Cole[150], A. Khan[150], P. Kyberd[150], I.D. Reid[150], S. Abdullin[151], A. Brinkerhoff[151], E. Collins[151], M.R. Darwish[151], J. Dittmann[151], K. Hatakeyama[151], V. Hegde[151], J. Hiltbrand[151], B. McMaster[151], J. Samudio[151], S. Sawant[151], C. Sutantawibul[151], J. Wilson[151], J.M. Hogan[152], R. Bartek[153], A. Dominguez[153], S. Raj[153], B. Sahu[153], A.E. Simsek[153], S.S. Yu[153], B. Bam[154], A. Buchot Perraguin[154], S. Campbell[154], R. Chudasama[154], S.I. Cooper[154], C. Crovella[154], G. Fidalgo[154], S.V. Gleyzer[154], A. Khukhunaishvili[154], K. Matchev[154], E. Pearson[154], P. Rumerio[154,bz], E. Usai[154], R. Yi[154], S. Cholak[155], G. De Castro[155], Z. Demiragli[155], C. Erice[155], C. Fangmeier[155], C. Fernandez Madrazo[155], J. Fulcher[155], F. Golf[155], S. Jeon[155], J. O'Cain[155], I. Reed[155], J. Rohlf[155], K. Salyer[155], D. Sperka[155], D. Spitzbart[155], I. Suarez[155], A. Tsatsos[155], E. Wurtz[155], A.G. Zecchinelli[155], G. Barone[156], G. Benelli[156], D. Cutts[156], S. Ellis[156], L. Gouskos[156], M. Hadley[156], U. Heintz[156], K.W. Ho[156], T. Kwon[156], L. Lambrecht[156], G. Landsberg[156], K.T. Lau[156], J. Luo[156], S. Mondal[156], J. Roloff[156], T. Russell[156], S. Sagir[156,ca], X. Shen[156], M. Stamenkovic[156], N. Venkatasubramanian[156], S. Abbott[157], S. Baradia[157], B. Barton[157], R. Breedon[157], H. Cai[157], M. Calderon De La Barca Sanchez[157], E. Cannaert[157], M. Chertok[157], M. Citron[157], J. Conway[157], P.T. Cox[157], F. Eble[157], R. Erbacher[157], O. Kukral[157], G. Mocellin[157], S. Ostrom[157], I. Salazar Segovia[157], J.S. Tafoya Vargas[157], W. Wei[157], S. Yoo[157], K. Adamidis[158], M. Bachtis[158], D. Campos[158], R. Cousins[158], S. Crossley[158], G. Flores Avila[158], J. Hauser[158], M. Ignatenko[158], M.A. Iqbal[158], T. Lam[158], Y.f. Lo[158], E. Manca[158], A. Nunez Del Prado[158], D. Saltzberg[158], V. Valuev[158], R. Clare[159], J.W. Gary[159], G. Hanson[159], A. Aportela[160], A. Arora[160], J.G. Branson[160], S. Cittolin[160], B. D'Anzi[160], D. Diaz[160], J. Duarte[160], L. Giannini[160], Y. Gu[160], J. Guiang[160], V. Krutelyov[160], R. Lee[160], J. Letts[160], H. Li[160], M. Masciovecchio[160], F. Mokhtar[160], S. Mukherjee[160], M. Pieri[160], D. Primosch[160], M. Quinnan[160], V. Sharma[160], M. Tadel[160], E. Vourliotis[160], F. Würthwein[160], A. Yagil[160], Z. Zhao[160], A. Barzdukas[161], L. Brennan[161], C. Campagnari[161], S. Carron Montero[161,cb], K. Downham[161], C. Grieco[161], M.M. Hussain[161], J. Incandela[161], M.W.K. Lai[161], A.J. Li[161], P. Masterson[161], J. Richman[161], S.N. Santpur[161], D. Stuart[161], T.Á. Vámi[161], X. Yan[161], D. Zhang[161], A. Albert[162], S. Bhattacharya[162], A. Bornheim[162], O. Cerri[162], R. Kansal[162], H.B. Newman[162], G. Reales Gutiérrez[162], T. Sievert[162], M. Spiropulu[162], C. Sun[162], J.R. Vlimant[162], R.A. Wynne[162], S. Xie[162], J. Alison[163], S. An[163], M. Cremonesi[163], V. Dutta[163], E.Y. Ertorer[163], T. Ferguson[163], T.A. Gómez Espinosa[163], A. Harilal[163], A. Kallil Tharayil[163], M. Kanemura[163], C. Liu[163], M. Marchegiani[163], P. Meiring[163], S. Murthy[163], P. Palit[163], K. Park[163], M. Paulini[163], A. Roberts[163], A. Sanchez[163], J.P. Cumalat[164], W.T. Ford[164], A. Hart[164], S. Kwan[164], J. Pearkes[164], C. Savard[164], N. Schonbeck[164], K. Stenson[164], K.A. Ulmer[164], S.R. Wagner[164], N. Zipper[164], D. Zuolo[164], J. Alexander[165], X. Chen[165], J. Dickinson[165], A. Duquette[165], J. Fan[165], X. Fan[165], J. Grassi[165], S. Hogan[165], P. Kotamnives[165], J. Monroy[165], G. Niendorf[165], M. Oshiro[165], J.R. Patterson[165], A. Ryd[165], J. Thom[165], H.A. Weber[165], B. Weiss[165], P. Wittich[165], R. Zou[165], L. Zygala[165], M. Albrow[166],

JHEP08(2026)098

M. Alyari[166], O. Amram[166], G. Apollinari[166], A. Apresyan[166], L.A.T. Bauerdick[166], D. Berry[166], J. Berryhill[166], P.C. Bhat[166], K. Burkett[166], J.N. Butler[166], A. Canepa[166], G.B. Cerati[166], H.W.K. Cheung[166], F. Chlebana[166], C. Cosby[166], G. Cummings[166], I. Dutta[166], V.D. Elvira[166], J. Freeman[166], A. Gandrakota[166], Z. Gecse[166], L. Gray[166], D. Green[166], A. Grummer[166], S. Grünendahl[166], D. Guerrero[166], O. Gutsche[166], R.M. Harris[166], J. Hirschauer[166], V. Innocente[166], B. Jayatilaka[166], S. Jindariani[166], M. Johnson[166], U. Joshi[166], R.S. Kim[166], B. Klima[166], S. Lammel[166], D. Lincoln[166], R. Lipton[166], T. Liu[166], K. Maeshima[166], D. Mason[166], P. McBride[166], P. Merkel[166], S. Mrenna[166], S. Nahn[166], J. Ngadiuba[166], D. Noonan[166], S. Norberg[166], V. Papadimitriou[166], N. Pastika[166], K. Pedro[166], C. Pena[166,cc], C.E. Perez Lara[166], V. Perovic[166], F. Ravera[166], A. Reinsvold Hall[166,cd], L. Ristori[166], M. Safdari[166], E. Sexton-Kennedy[166], E. Smith[166], N. Smith[166], A. Soha[166], L. Spiegel[166], S. Stoynev[166], J. Strait[166], L. Taylor[166], S. Tkaczyk[166], N.V. Tran[166], L. Uplegger[166], E.W. Vaandering[166], C. Wang[166], I. Zoi[166], C. Aruta[167], P. Avery[167], D. Bourilkov[167], P. Chang[167], V. Cherepanov[167], R.D. Field[167], C. Huh[167], E. Koenig[167], M. Kolosova[167], J. Konigsberg[167], A. Korytov[167], G. Mitselmakher[167], K. Mohrman[167], A. Muthirakalayil Madhu[167], N. Rawal[167], S. Rosenzweig[167], V. Sulimov[167], Y. Takahashi[167], J. Wang[167], T. Adams[168], A. Al Kadhim[168], A. Askew[168], S. Bower[168], R. Goff[168], R. Hashmi[168], A. Hassani[168], T. Kolberg[168], G. Martinez[168], M. Mazza[168], H. Prosper[168], P.R. Prova[168], R. Yohay[168], B. Alsufyani[169], S. Butalla[169], S. Das[169], M. Hohlmann[169], M. Lavinsky[169], E. Yanes[169], M.R. Adams[170], N. Barnett[170], A. Baty[170], C. Bennett[170], R. Cavanaugh[170], R. Escobar Franco[170], O. Evdokimov[170], C.E. Gerber[170], H. Gupta[170], M. Hawksworth[170], A. Hingrajiya[170], D.J. Hofman[170], Z. Huang[170], J.h. Lee[170], C. Mills[170], S. Nanda[170], G. Nigmatkulov[170], B. Ozek[170], T. Phan[170], D. Pilipovic[170], R. Pradhan[170], E. Prifti[170], P. Roy[170], T. Roy[170], D. Shekar[170], N. Singh[170], A. Thielen[170], M.B. Tonjes[170], N. Varelas[170], M.A. Wadud[170], J. Yoo[170], M. Alhusseini[171], D. Blend[171], K. Dilsiz[171,ce], O.K. Köseyan[171], A. Mestvirishvili[171,cf], O. Neogi[171], H. Ogul[171,cg], Y. Onel[171], A. Penzo[171], C. Snyder[171], E. Tiras[171,ch], B. Blumenfeld[172], J. Davis[172], A.V. Gritsan[172], L. Kang[172], S. Kyriacou[172], P. Maksimovic[172], M. Roguljic[172], S. Sekhar[172], M.V. Srivastav[172], M. Swartz[172], A. Abreu[173], L.F. Alcerro Alcerro[173], J. Anguiano[173], S. Arteaga Escatel[173], P. Baringer[173], A. Bean[173], R. Bhattacharya[173], Z. Flowers[173], D. Grove[173], J. King[173], G. Krintiras[173], M. Lazarovits[173], C. Le Mahieu[173], J. Marquez[173], M. Murray[173], M. Nickel[173], S. Popescu[173,ci], C. Rogan[173], C. Royon[173], S. Rudrabhatla[173], S. Sanders[173], C. Smith[173], G. Wilson[173], B. Allmond[174], N. Islam[174], A. Ivanov[174], K. Kaadze[174], Y. Maravin[174], J. Natoli[174], G.G. Reddy[174], D. Roy[174], G. Sorrentino[174], A. Baden[175], A. Belloni[175], J. Bistany-riebman[175], S.C. Eno[175], N.J. Hadley[175], S. Jabeen[175], R.G. Kellogg[175], T. Koeth[175], B. Kronheim[175], S. Lascio[175], P. Major[175], A.C. Mignerey[175], C. Palmer[175], C. Papageorgakis[175], M.M. Paranjpe[175], E. Popova[175,cj], A. Shevelev[175], L. Zhang[175], C. Baldenegro Barrera[176], H. Bossi[176], S. Bright-Thonney[176], I.A. Cali[176], Y.c. Chen[176], P.c. Chou[176], M. D'Alfonso[176], J. Eysermans[176], C. Freer[176], G. Gomez-Ceballos[176], M. Goncharov[176], G. Grosso[176], P. Harris[176], D. Hoang[176], G.M. Innocenti[176], K. Ivanov[176], G. Kopp[176], D. Kovalskyi[176], L. Lavezzo[176],

JHEP08(2026)098

Y.-J. Lee[176], K. Long[176], C. Mcginn[176], A. Novak[176], M.I. Park[176], C. Paus[176], C. Reissel[176], C. Roland[176], G. Roland[176], S. Rothman[176], T.a. Sheng[176], G.S.F. Stephans[176], D. Walter[176], J. Wang[176], Z. Wang[176], B. Wyslouch[176], T. J. Yang[176], A. Alpana[177], B. Crossman[177], W.J. Jackson[177], C. Kapsiak[177], M. Krohn[177], D. Mahon[177], J. Mans[177], B. Marzocchi[177], R. Rusack[177], O. Sancar[177], R. Saradhy[177], N. Strobbe[177], K. Bloom[178], D.R. Claes[178], G. Haza[178], J. Hossain[178], C. Joo[178], I. Kravchenko[178], K.H.M. Kwok[178], A. Rohilla[178], J.E. Siado[178], W. Tabb[178], A. Vagnerini[178], A. Wightman[178], H. Bandyopadhyay[179], L. Hay[179], H.w. Hsia[179], I. Iashvili[179], A. Kalogeropoulos[179], A. Kharchilava[179], A. Mandal[179], M. Morris[179], D. Nguyen[179], O. Poncet[179], S. Rappoccio[179], H. Rejeb Sfar[179], W. Terrill[179], A. Williams[179], D. Yu[179], A. Aarif[180], G. Alverson[180], E. Barberis[180], J. Bonilla[180], B. Bylsma[180], M. Campana[180], J. Dervan[180], Y. Haddad[180], Y. Han[180], I. Israr[180], A. Krishna[180], M. Lu[180], N. Manganelli[180], R. Mccarthy[180], D.M. Morse[180], T. Orimoto[180], L. Skinnari[180], C.S. Thoreson[180], E. Tsai[180], D. Wood[180], S. Dittmer[181], K.A. Hahn[181], M. Mcginnis[181], Y. Miao[181], D.G. Monk[181], M.H. Schmitt[181], A. Taliercio[181], M. Velasco[181], J. Wang[181], G. Agarwal[182], R. Band[182], R. Bucci[182], S. Castells[182], A. Das[182], A. Datta[182], A. Ehnis[182], R. Goldouzian[182], M. Hildreth[182], K. Hurtado Anampa[182], T. Ivanov[182], C. Jessop[182], A. Karneyeu[182], K. Lannon[182], J. Lawrence[182], N. Loukas[182], L. Lutton[182], J. Mariano[182], N. Marinelli[182], P. Mastrapasqua[182], T. McCauley[182], C. Mcgrady[182], C. Moore[182], Y. Musienko[182,ck], H. Nelson[182], M. Osherson[182], A. Piccinelli[182], R. Ruchti[182], A. Townsend[182], Y. Wan[182], M. Wayne[182], H. Yockey[182], M. Carrigan[183], R. De Los Santos[183], L.S. Durkin[183], C. Hill[183], M. Joyce[183], D.A. Wenzl[183], B.L. Winer[183], B. R. Yates[183], H. Bouchamaoui[184], G. Dezoort[184], P. Elmer[184], A. Frankenthal[184], M. Galli[184], B. Greenberg[184], N. Haubrich[184], K. Kennedy[184], Y. Lai[184], D. Lange[184], A. Loeliger[184], D. Marlow[184], I. Ojalvo[184], J. Olsen[184], F. Simpson[184], D. Stickland[184], C. Tully[184], S. Malik[185], R. Sharma[185], S. Chandra[186], A. Gu[186], L. Gutay[186], M. Huwiler[186], M. Jones[186], A.W. Jung[186], D. Kondratyev[186], J. Li[186], M. Liu[186], M. Macedo[186], G. Negro[186], N. Neumeister[186], G. Paspalaki[186], S. Piperov[186], N.R. Saha[186], J.F. Schulte[186], F. Wang[186], A. Wildridge[186], W. Xie[186], Y. Yao[186], Y. Zhong[186], N. Parashar[187], A. Pathak[187], E. Shumka[187], D. Acosta[188], A. Agrawal[188], C. Arbour[188], T. Carnahan[188], K.M. Ecklund[188], F.J.M. Geurts[188], T. Huang[188], I. Krommydas[188], N. Lewis[188], W. Li[188], J. Lin[188], O. Miguel Colin[188], B.P. Padley[188], R. Redjimi[188], J. Rotter[188], C. Vico Villalba[188], M. Wulansatiti[188], E. Yigitbasi[188], Y. Zhang[188], O. Bessidskaia Bylund[189], A. Bodek[189], P. de Barbaro[189,†], R. Demina[189], A. Garcia-Bellido[189], H.S. Hare[189], O. Hindrichs[189], N. Parmar[189], P. Parygin[189,cj], H. Seo[189], R. Taus[189], Y.h. Yu[189], B. Chiarito[190], J.P. Chou[190], S.V. Clark[190], S. Donnelly[190], D. Gadkari[190], Y. Gershtein[190], E. Halkiadakis[190], C. Houghton[190], D. Jaroslawski[190], A. Kobert[190], I. Laflotte[190], A. Lath[190], J. Martins[190], M. Perez Prada[190], B. Rand[190], J. Reichert[190], P. Saha[190], S. Salur[190], S. Somalwar[190], R. Stone[190], S.A. Thayil[190], S. Thomas[190], J. Vora[190], D. Ally[191], A.G. Delannoy[191], S. Fiorendi[191], J. Harris[191], T. Holmes[191], A.R. Kanuganti[191], N. Karunarathna[191], J. Lawless[191], L. Lee[191], E. Nibigira[191], B. Skipworth[191], S. Spanier[191], D. Aebi[192],

JHEP08(2026)098

M. Ahmad[192], T. Akhter[192], K. Androsov[192], A. Basnet[192], A. Bolshov[192], O. Bouhali[192,cl], A. Cagnotta[192], S. Cooperstein[192], V. D'Amante[192], R. Eusebi[192], P. Flanagan[192], J. Gilmore[192], Y. Guo[192], T. Kamon[192], S. Luo[192], R. Mueller[192], A. Safonov[192], N. Akchurin[193], J. Damgov[193], Y. Feng[193], N. Gogate[193], W. Jin[193], S.W. Lee[193], C. Madrid[193], A. Mankel[193], T. Peltola[193], I. Volobouev[193], E. Appelt[194], Y. Chen[194], S. Greene[194], A. Gurrola[194], W. Johns[194], R. Kunnawalkam Elayavalli[194], A. Melo[194], D. Rathjens[194], F. Romeo[194], P. Sheldon[194], S. Tuo[194], J. Velkovska[194], J. Viinikainen[194], J. Zhang[194], B. Cardwell[195], H. Chung[195], B. Cox[195], J. Hakala[195], G. Hamilton Ilha Machado[195], R. Hirosky[195], M. Jose[195], A. Ledovskoy[195], C. Mantilla[195], C. Neu[195], C. Ramón Álvarez[195], Z. Wu[195], S. Bhattacharya[196], P.E. Karchin[196], A. Aravind[197], S. Banerjee[197], K. Black[197], T. Bose[197], E. Chavez[197], S. Dasu[197], P. Everaerts[197], C. Galloni[197], H. He[197], M. Herndon[197], A. Herve[197], C.K. Koraka[197], S. Lomte[197], R. Loveless[197], A. Mallampalli[197], A. Mohammadi[197], S. Mondal[197], T. Nelson[197], G. Parida[197], L. Pétré[197], D. Pinna[197], A. Savin[197], V. Shang[197], V. Sharma[197], R. Simeon[197], W.H. Smith[197], D. Teague[197], A. Warden[197], S. Afanasiev[198], V. Alexakhin[198], Yu. Andreev[198], T. Aushev[198], D. Budkouski[198], R. Chistov[198], M. Danilov[198], T. Dimova[198], A. Ershov[198], S. Gninenko[198], I. Gorbunov[198], A. Kamenev[198], V. Karjavine[198], M. Kirsanov[198], V. Klyukhin[198], O. Kodolova[198,cm], V. Korenkov[198], I. Korsakov[198], A. Kozyrev[198], N. Krasnikov[198], A. Lanev[198], A. Malakhov[198], V. Matveev[198], A. Nikitenko[198,cn,co], V. Palichik[198], V. Perelygin[198], S. Petrushanko[198], O. Radchenko[198], M. Savina[198], V. Shalaev[198], S. Shmatov[198], S. Shulha[198], Y. Skovpen[198], K. Slizhevskiy[198], V. Smirnov[198], O. Teryaev[198], I. Tlisova[198], A. Toropin[198], N. Voytishin[198], A. Zarubin[198], I. Zhizhin[198], E. Boos[199], V. Bunichev[199], M. Dubinin[199,cc], L. Dudko[199], A. Gribushin[199], V. Kim[199,ck], V. Murzin[199], V. Oreshkin[199], V. Savrin[199], A. Snigirev[199], D. Sosnov[199]

[1] *Yerevan Physics Institute, Yerevan, Armenia*
[2] *Institut für Hochenergiephysik, Vienna, Austria*
[3] *Universiteit Antwerpen, Antwerpen, Belgium*
[4] *Vrije Universiteit Brussel, Brussel, Belgium*
[5] *Université Libre de Bruxelles, Bruxelles, Belgium*
[6] *Ghent University, Ghent, Belgium*
[7] *Université Catholique de Louvain, Louvain-la-Neuve, Belgium*
[8] *Centro Brasileiro de Pesquisas Fisicas, Rio de Janeiro, Brazil*
[9] *Universidade do Estado do Rio de Janeiro, Rio de Janeiro, Brazil*
[10] *Universidade Estadual Paulista, Universidade Federal do ABC, São Paulo, Brazil*
[11] *Institute for Nuclear Research and Nuclear Energy, Bulgarian Academy of Sciences, Sofia, Bulgaria*
[12] *University of Sofia, Sofia, Bulgaria*
[13] *Instituto De Alta Investigación, Universidad de Tarapacá, Casilla 7 D, Arica, Chile*
[14] *Universidad Tecnica Federico Santa Maria, Valparaiso, Chile*
[15] *Beihang University, Beijing, China*
[16] *Department of Physics, Tsinghua University, Beijing, China*
[17] *Institute of High Energy Physics, Beijing, China*
[18] *State Key Laboratory of Nuclear Physics and Technology, Peking University, Beijing, China*
[19] *State Key Laboratory of Nuclear Physics and Technology, Institute of Quantum Matter, South China Normal University, Guangzhou, China*
[20] *Sun Yat-Sen University, Guangzhou, China*
[21] *University of Science and Technology of China, Hefei, China*

JHEP08(2026)098

[22] Nanjing Normal University, Nanjing, China
[23] Institute of Frontier and Interdisciplinary Science, Shandong University, Qingdao, China
[24] Institute of Modern Physics and Key Laboratory of Nuclear Physics and Ion-beam Application (MOE) - Fudan University, Shanghai, China
[25] Zhejiang University, Hangzhou, Zhejiang, China
[26] Universidad de Los Andes, Bogota, Colombia
[27] Universidad de Antioquia, Medellin, Colombia
[28] University of Split, Faculty of Electrical Engineering, Mechanical Engineering and Naval Architecture, Split, Croatia
[29] University of Split, Faculty of Science, Split, Croatia
[30] Institute Rudjer Boskovic, Zagreb, Croatia
[31] University of Cyprus, Nicosia, Cyprus
[32] Charles University, Prague, Czech Republic
[33] Universidad San Francisco de Quito, Quito, Ecuador
[34] Academy of Scientific Research and Technology of the Arab Republic of Egypt, Egyptian Network of High Energy Physics, Cairo, Egypt
[35] Center for High Energy Physics (CHEP-FU), Fayoum University, El-Fayoum, Egypt
[36] National Institute of Chemical Physics and Biophysics, Tallinn, Estonia
[37] Department of Physics, University of Helsinki, Helsinki, Finland
[38] Helsinki Institute of Physics, Helsinki, Finland
[39] Lappeenranta-Lahti University of Technology, Lappeenranta, Finland
[40] IRFU, CEA, Université Paris-Saclay, Gif-sur-Yvette, France
[41] Laboratoire Leprince-Ringuet, CNRS/IN2P3, Ecole Polytechnique, Institut Polytechnique de Paris, Palaiseau, France
[42] Université de Strasbourg, CNRS, IPHC UMR 7178, Strasbourg, France
[43] Centre de Calcul de l'Institut National de Physique Nucleaire et de Physique des Particules, CNRS/IN2P3, Villeurbanne, France
[44] Institut de Physique des 2 Infinis de Lyon (IP2I), Villeurbanne, France
[45] Georgian Technical University, Tbilisi, Georgia
[46] RWTH Aachen University, I. Physikalisches Institut, Aachen, Germany
[47] RWTH Aachen University, III. Physikalisches Institut A, Aachen, Germany
[48] RWTH Aachen University, III. Physikalisches Institut B, Aachen, Germany
[49] Deutsches Elektronen-Synchrotron, Hamburg, Germany
[50] University of Hamburg, Hamburg, Germany
[51] Karlsruher Institut fuer Technologie, Karlsruhe, Germany
[52] Institute of Nuclear and Particle Physics (INPP), NCSR Demokritos, Aghia Paraskevi, Greece
[53] National and Kapodistrian University of Athens, Athens, Greece
[54] National Technical University of Athens, Athens, Greece
[55] University of Ioánnina, Ioánnina, Greece
[56] HUN-REN Wigner Research Centre for Physics, Budapest, Hungary
[57] MTA-ELTE Lendület CMS Particle and Nuclear Physics Group, Eötvös Loránd University, Budapest, Hungary
[58] Faculty of Informatics, University of Debrecen, Debrecen, Hungary
[59] HUN-REN ATOMKI - Institute of Nuclear Research, Debrecen, Hungary
[60] Karoly Robert Campus, MATE Institute of Technology, Gyongyos, Hungary
[61] IIT Bhubaneswar, Bhubaneswar, India
[62] Panjab University, Chandigarh, India
[63] University of Delhi, Delhi, India
[64] Indian Institute of Technology Mandi (IIT-Mandi), Himachal Pradesh, India
[65] University of Hyderabad, Hyderabad, India
[66] Indian Institute of Technology Kanpur, Kanpur, India
[67] Saha Institute of Nuclear Physics, HBNI, Kolkata, India
[68] Indian Institute of Technology Madras, Madras, India

JHEP08(2026)098

[69] IISER Mohali, India, Mohali, India
[70] Tata Institute of Fundamental Research-A, Mumbai, India
[71] Tata Institute of Fundamental Research-B, Mumbai, India
[72] National Institute of Science Education and Research, An OCC of Homi Bhabha National Institute, Bhubaneswar, Odisha, India
[73] Indian Institute of Science Education and Research (IISER), Pune, India
[74] Indian Institute of Technology Hyderabad, Telangana, India
[75] Isfahan University of Technology, Isfahan, Iran
[76] Institute for Research in Fundamental Sciences (IPM), Tehran, Iran
[77] University College Dublin, Dublin, Ireland
[78a] INFN Sezione di Bari, Bari, Italy
[78b] Università di Bari, Bari, Italy
[78c] Politecnico di Bari, Bari, Italy
[79a] INFN Sezione di Bologna, Bologna, Italy
[79b] Università di Bologna, Bologna, Italy
[80a] INFN Sezione di Catania, Catania, Italy
[80b] Università di Catania, Catania, Italy
[81a] INFN Sezione di Firenze, Firenze, Italy
[81b] Università di Firenze, Firenze, Italy
[82] INFN Laboratori Nazionali di Frascati, Frascati, Italy
[83a] INFN Sezione di Genova, Genova, Italy
[83b] Università di Genova, Genova, Italy
[84a] INFN Sezione di Milano-Bicocca, Milano, Italy
[84b] Università di Milano-Bicocca, Milano, Italy
[85a] INFN Sezione di Napoli, Napoli, Italy
[85b] Università di Napoli 'Federico II', Napoli, Italy
[85c] Università della Basilicata, Potenza, Italy
[85d] Scuola Superiore Meridionale (SSM), Napoli, Italy
[86a] INFN Sezione di Padova, Padova, Italy
[86b] Università di Padova, Padova, Italy
[86c] Universita degli Studi di Cagliari, Cagliari, Italy
[87a] INFN Sezione di Pavia, Pavia, Italy
[87b] Università di Pavia, Pavia, Italy
[88a] INFN Sezione di Perugia, Perugia, Italy
[88b] Università di Perugia, Perugia, Italy
[89a] INFN Sezione di Pisa, Pisa, Italy
[89b] Università di Pisa, Pisa, Italy
[89c] Scuola Normale Superiore di Pisa, Pisa, Italy
[89d] Università di Siena, Siena, Italy
[90a] INFN Sezione di Roma, Roma, Italy
[90b] Sapienza Università di Roma, Roma, Italy
[91a] INFN Sezione di Torino, Torino, Italy
[91b] Università di Torino, Torino, Italy
[91c] Università del Piemonte Orientale, Novara, Italy
[92a] INFN Sezione di Trieste, Trieste, Italy
[92b] Università di Trieste, Trieste, Italy
[93] Kyungpook National University, Daegu, Korea
[94] Department of Mathematics and Physics - GWNU, Gangneung, Korea
[95] Chonnam National University, Institute for Universe and Elementary Particles, Kwangju, Korea
[96] Hanyang University, Seoul, Korea
[97] Korea University, Seoul, Korea
[98] Kyung Hee University, Department of Physics, Seoul, Korea
[99] Sejong University, Seoul, Korea

JHEP08(2026)098

[100] Seoul National University, Seoul, Korea
[101] University of Seoul, Seoul, Korea
[102] Yonsei University, Department of Physics, Seoul, Korea
[103] Sungkyunkwan University, Suwon, Korea
[104] College of Engineering and Technology, American University of the Middle East (AUM), Dasman, Kuwait
[105] Kuwait University - College of Science - Department of Physics, Safat, Kuwait
[106] Riga Technical University, Riga, Latvia
[107] University of Latvia (LU), Riga, Latvia
[108] Vilnius University, Vilnius, Lithuania
[109] National Centre for Particle Physics, Universiti Malaya, Kuala Lumpur, Malaysia
[110] Universidad de Sonora (UNISON), Hermosillo, Mexico
[111] Centro de Investigacion y de Estudios Avanzados del IPN, Mexico City, Mexico
[112] Universidad Iberoamericana, Mexico City, Mexico
[113] Benemerita Universidad Autonoma de Puebla, Puebla, Mexico
[114] University of Montenegro, Podgorica, Montenegro
[115] University of Canterbury, Christchurch, New Zealand
[116] National Centre for Physics, Quaid-I-Azam University, Islamabad, Pakistan
[117] AGH University of Krakow, Krakow, Poland
[118] National Centre for Nuclear Research, Swierk, Poland
[119] Institute of Experimental Physics, Faculty of Physics, University of Warsaw, Warsaw, Poland
[120] Warsaw University of Technology, Warsaw, Poland
[121] Laboratório de Instrumentação e Física Experimental de Partículas, Lisboa, Portugal
[122] Faculty of Physics, University of Belgrade, Belgrade, Serbia
[123] VINCA Institute of Nuclear Sciences, University of Belgrade, Belgrade, Serbia
[124] Centro de Investigaciones Energéticas Medioambientales y Tecnológicas (CIEMAT), Madrid, Spain
[125] Universidad Autónoma de Madrid, Madrid, Spain
[126] Universidad de Oviedo, Instituto Universitario de Ciencias y Tecnologías Espaciales de Asturias (ICTEA), Oviedo, Spain
[127] Instituto de Física de Cantabria (IFCA), CSIC-Universidad de Cantabria, Santander, Spain
[128] University of Colombo, Colombo, Sri Lanka
[129] University of Ruhuna, Department of Physics, Matara, Sri Lanka
[130] CERN, European Organization for Nuclear Research, Geneva, Switzerland
[131] PSI Center for Neutron and Muon Sciences, Villigen, Switzerland
[132] ETH Zurich - Institute for Particle Physics and Astrophysics (IPA), Zurich, Switzerland
[133] Universität Zürich, Zurich, Switzerland
[134] National Central University, Chung-Li, Taiwan
[135] National Taiwan University (NTU), Taipei, Taiwan
[136] High Energy Physics Research Unit, Department of Physics, Faculty of Science, Chulalongkorn University, Bangkok, Thailand
[137] Tunis El Manar University, Tunis, Tunisia
[138] Çukurova University, Physics Department, Science and Art Faculty, Adana, Turkey
[139] Hacettepe University, Ankara, Turkey
[140] Middle East Technical University, Physics Department, Ankara, Turkey
[141] Bogazici University, Istanbul, Turkey
[142] Istanbul Technical University, Istanbul, Turkey
[143] Istanbul University, Istanbul, Turkey
[144] Yildiz Technical University, Istanbul, Turkey
[145] Institute for Scintillation Materials of National Academy of Science of Ukraine, Kharkiv, Ukraine
[146] National Science Centre, Kharkiv Institute of Physics and Technology, Kharkiv, Ukraine
[147] University of Bristol, Bristol, U.K.
[148] Rutherford Appleton Laboratory, Didcot, U.K.
[149] Imperial College, London, U.K.
[150] Brunel University, Uxbridge, U.K.

JHEP08(2026)098

[151] *Baylor University, Waco, Texas, U.S.A.*
[152] *Bethel University, St. Paul, Minnesota, U.S.A.*
[153] *Catholic University of America, Washington, DC, U.S.A.*
[154] *The University of Alabama, Tuscaloosa, Alabama, U.S.A.*
[155] *Boston University, Boston, Massachusetts, U.S.A.*
[156] *Brown University, Providence, Rhode Island, U.S.A.*
[157] *University of California, Davis, Davis, California, U.S.A.*
[158] *University of California, Los Angeles, California, U.S.A.*
[159] *University of California, Riverside, Riverside, California, U.S.A.*
[160] *University of California, San Diego, La Jolla, California, U.S.A.*
[161] *University of California, Santa Barbara - Department of Physics, Santa Barbara, California, U.S.A.*
[162] *California Institute of Technology, Pasadena, California, U.S.A.*
[163] *Carnegie Mellon University, Pittsburgh, Pennsylvania, U.S.A.*
[164] *University of Colorado Boulder, Boulder, Colorado, U.S.A.*
[165] *Cornell University, Ithaca, New York, U.S.A.*
[166] *Fermi National Accelerator Laboratory, Batavia, Illinois, U.S.A.*
[167] *University of Florida, Gainesville, Florida, U.S.A.*
[168] *Florida State University, Tallahassee, Florida, U.S.A.*
[169] *Florida Institute of Technology, Melbourne, Florida, U.S.A.*
[170] *University of Illinois Chicago, Chicago, Illinois, U.S.A.*
[171] *The University of Iowa, Iowa City, Iowa, U.S.A.*
[172] *Johns Hopkins University, Baltimore, Maryland, U.S.A.*
[173] *The University of Kansas, Lawrence, Kansas, U.S.A.*
[174] *Kansas State University, Manhattan, Kansas, U.S.A.*
[175] *University of Maryland, College Park, Maryland, U.S.A.*
[176] *Massachusetts Institute of Technology, Cambridge, Massachusetts, U.S.A.*
[177] *University of Minnesota, Minneapolis, Minnesota, U.S.A.*
[178] *University of Nebraska-Lincoln, Lincoln, Nebraska, U.S.A.*
[179] *State University of New York at Buffalo, Buffalo, New York, U.S.A.*
[180] *Northeastern University, Boston, Massachusetts, U.S.A.*
[181] *Northwestern University, Evanston, Illinois, U.S.A.*
[182] *University of Notre Dame, Notre Dame, Indiana, U.S.A.*
[183] *The Ohio State University, Columbus, Ohio, U.S.A.*
[184] *Princeton University, Princeton, New Jersey, U.S.A.*
[185] *University of Puerto Rico, Mayaguez, Puerto Rico, U.S.A.*
[186] *Purdue University, West Lafayette, Indiana, U.S.A.*
[187] *Purdue University Northwest, Hammond, Indiana, U.S.A.*
[188] *Rice University, Houston, Texas, U.S.A.*
[189] *University of Rochester, Rochester, New York, U.S.A.*
[190] *Rutgers, The State University of New Jersey, Piscataway, New Jersey, U.S.A.*
[191] *University of Tennessee, Knoxville, Tennessee, U.S.A.*
[192] *Texas A&M University, College Station, Texas, U.S.A.*
[193] *Texas Tech University, Lubbock, Texas, U.S.A.*
[194] *Vanderbilt University, Nashville, Tennessee, U.S.A.*
[195] *University of Virginia, Charlottesville, Virginia, U.S.A.*
[196] *Wayne State University, Detroit, Michigan, U.S.A.*
[197] *University of Wisconsin - Madison, Madison, Wisconsin, U.S.A.*
[198] *An institute or international laboratory covered by a cooperation agreement with CERN*
[199] *An institute formerly covered by a cooperation agreement with CERN*

[a] *Also at Yerevan State University, Yerevan, Armenia*
[b] *Also at TU Wien, Vienna, Austria*
[c] *Also at Ghent University, Ghent, Belgium*

JHEP08(2026)098

[d] Also at FACAMP - Faculdades de Campinas, Sao Paulo, Brazil
[e] Also at Universidade Estadual de Campinas, Campinas, Brazil
[f] Also at Federal University of Rio Grande do Sul, Porto Alegre, Brazil
[g] Also at The University of the State of Amazonas, Manaus, Brazil
[h] Also at University of Chinese Academy of Sciences, Beijing, China
[i] Also at University of Chinese Academy of Sciences, Beijing, China
[j] Also at School of Physics, Zhengzhou University, Zhengzhou, China
[k] Now at Henan Normal University, Xinxiang, China
[l] Also at University of Shanghai for Science and Technology, Shanghai, China
[m] Also at The University of Iowa, Iowa City, Iowa, U.S.A.
[n] Also at Nanjing Normal University, Nanjing, China
[o] Also at Center for High Energy Physics, Peking University, Beijing, China
[p] Also at Helwan University, Cairo, Egypt
[q] Now at Zewail City of Science and Technology, Zewail, Egypt
[r] Also at Cairo University, Cairo, Egypt
[s] Also at Université de Haute Alsace, Mulhouse, France
[t] Also at Purdue University, West Lafayette, Indiana, U.S.A.
[u] Also at Another institute or international laboratory covered by a cooperation agreement with CERN
[v] Also at University of Hamburg, Hamburg, Germany
[w] Also at RWTH Aachen University, III. Physikalisches Institut A, Aachen, Germany
[x] Also at Bergische University Wuppertal (BUW), Wuppertal, Germany
[y] Also at Brandenburg University of Technology, Cottbus, Germany
[z] Also at Forschungszentrum Jülich, Juelich, Germany
[aa] Now at RWTH Aachen University, III. Physikalisches Institut A, Aachen, Germany
[ab] Also at CERN, European Organization for Nuclear Research, Geneva, Switzerland
[ac] Also at HUN-REN ATOMKI - Institute of Nuclear Research, Debrecen, Hungary
[ad] Now at Universitatea Babes-Bolyai - Facultatea de Fizica, Cluj-Napoca, Romania
[ae] Also at MTA-ELTE Lendület CMS Particle and Nuclear Physics Group, Eötvös Loránd University, Budapest, Hungary
[af] Also at HUN-REN Wigner Research Centre for Physics, Budapest, Hungary
[ag] Also at Physics Department, Faculty of Science, Assiut University, Assiut, Egypt
[ah] Also at The University of Kansas, Lawrence, Kansas, U.S.A.
[ai] Also at Punjab Agricultural University, Ludhiana, India
[aj] Also at University of Hyderabad, Hyderabad, India
[ak] Also at Indian Institute of Science (IISc), Bangalore, India
[al] Also at University of Visva-Bharati, Santiniketan, India
[am] Also at Institute of Physics, Bhubaneswar, India
[an] Also at Deutsches Elektronen-Synchrotron, Hamburg, Germany
[ao] Also at Isfahan University of Technology, Isfahan, Iran
[ap] Also at Sharif University of Technology, Tehran, Iran
[aq] Also at Department of Physics, University of Science and Technology of Mazandaran, Behshahr, Iran
[ar] Also at Department of Physics, Faculty of Science, Arak University, ARAK, Iran
[as] Also at Italian National Agency for New Technologies, Energy and Sustainable Economic Development, Bologna, Italy
[at] Also at Centro Siciliano di Fisica Nucleare e di Struttura Della Materia, Catania, Italy
[au] Also at James Madison University, Harrisonburg, N/A, U.S.A.
[av] Also at Università degli Studi Guglielmo Marconi, Roma, Italy
[aw] Also at Scuola Superiore Meridionale, Università di Napoli 'Federico II', Napoli, Italy
[ax] Also at Fermi National Accelerator Laboratory, Batavia, Illinois, U.S.A.
[ay] Also at Lulea University of Technology, Lulea, Sweden
[az] Also at Consiglio Nazionale delle Ricerche - Istituto Officina dei Materiali, Perugia, Italy
[ba] Also at UPES - University of Petroleum and Energy Studies, Dehradun, India
[bb] Also at Institut de Physique des 2 Infinis de Lyon (IP2I), Villeurbanne, France

JHEP08(2026)098

[bc] Also at Department of Applied Physics, Faculty of Science and Technology, Universiti Kebangsaan Malaysia, Bangi, Malaysia
[bd] Also at Trincomalee Campus, Eastern University, Sri Lanka, Nilaveli, Sri Lanka
[be] Also at Saegis Campus, Nugegoda, Sri Lanka
[bf] Also at National and Kapodistrian University of Athens, Athens, Greece
[bg] Also at Ecole Polytechnique Fédérale Lausanne, Lausanne, Switzerland
[bh] Also at Universität Zürich, Zurich, Switzerland
[bi] Also at Stefan Meyer Institute for Subatomic Physics, Vienna, Austria
[bj] Also at Near East University, Research Center of Experimental Health Science, Mersin, Turkey
[bk] Also at Konya Technical University, Konya, Turkey
[bl] Also at Istanbul Topkapi University, Istanbul, Turkey
[bm] Also at Izmir Bakircay University, Izmir, Turkey
[bn] Also at Adiyaman University, Adiyaman, Turkey
[bo] Also at Bozok Universitetesi Rektörlügü, Yozgat, Turkey
[bp] Also at Istanbul Sabahattin Zaim University, Istanbul, Turkey
[bq] Also at Marmara University, Istanbul, Turkey
[br] Also at Milli Savunma University, Istanbul, Turkey
[bs] Also at Informatics and Information Security Research Center, Gebze/Kocaeli, Turkey
[bt] Also at Kafkas University, Kars, Turkey
[bu] Now at Istanbul Okan University, Istanbul, Turkey
[bv] Also at Istanbul University - Cerrahpasa, Faculty of Engineering, Istanbul, Turkey
[bw] Also at Istinye University, Istanbul, Turkey
[bx] Also at School of Physics and Astronomy, University of Southampton, Southampton, U.K.
[by] Also at Monash University, Faculty of Science, Clayton, Australia
[bz] Also at Università di Torino, Torino, Italy
[ca] Also at Karamanoğlu Mehmetbey University, Karaman, Turkey
[cb] Also at California Lutheran University, Thousand Oaks, California, U.S.A.
[cc] Also at California Institute of Technology, Pasadena, California, U.S.A.
[cd] Also at United States Naval Academy, Annapolis, Maryland, U.S.A.
[ce] Also at Bingol University, Bingol, Turkey
[cf] Also at Georgian Technical University, Tbilisi, Georgia
[cg] Also at Sinop University, Sinop, Turkey
[ch] Also at Erciyes University, Kayseri, Turkey
[ci] Also at Horia Hulubei National Institute of Physics and Nuclear Engineering (IFIN-HH), Bucharest, Romania
[cj] Now at Another institute formerly covered by a cooperation agreement with CERN
[ck] Also at Another institute formerly covered by a cooperation agreement with CERN
[cl] Also at Hamad Bin Khalifa University (HBKU), Doha, Qatar
[cm] Also at Yerevan Physics Institute, Yerevan, Armenia
[cn] Also at Imperial College, London, U.K.
[co] Now at Yerevan Physics Institute, Yerevan, Armenia
[†] Deceased

JHEP08(2026)098